Confining Cu(I) Ions within an Ir(III)-Based Twin-Cavity Cage for Photo-Triggered Dioxygen Activation toward C(sp^3)−H Oxidation

Zhuolin Shi,[a,c] Yuwen Wang,[c] Rong Zhang,[c] Hanshu Li,[b] Rui Cai,[d] Jinguo Wu,[c] Xin Wang,[c] Hechuan Li,[c] Xuezhao Li,*[a,b] Cheng He[c]

a. *Cancer Hospital of Dalian University of Technology, Dalian University of Technology, Shenyang, 110042, China.*
b. School of Chemistry, Dalian University of Technology, Dalian, 116024, China.
c. State Key Laboratory of Fine Chemicals, School of Chemical Engineering, Dalian University of Technology, Dalian, 116024, China.
d. Instrumental Analysis Center, Dalian University of Technology, Dalian, 116024, China.

Table of Contents

1. Materials and Instruments

Unless stated otherwise, all chemicals were of reagent grade quality obtained from commercial sources and used without further purification. Solvents (CH_3CN, CH_3OH, CH_2Cl_2, Toluene) were dried using a commercial solvent purification system (SG Water, Inc.). All reactions were carried out under a nitrogen or argon atmosphere, unless stated otherwise.

Nuclear magnetic resonance (NMR) spectra were recorded on a BRUKER 400 MHz spectrometer at 298 K. The following abbreviations were used to identify signal multiplicities: s, singlet; d, doublet; t, triplet; b, broad peaks; m, multiplet or overlapping peaks.

MALDI-TOF mass spectra were performed on Bruker ultraflexetreme spectrometer using methanol as mobile phase.

ESI-TOF mass spectra were carried out on a Waters Synapt G2-Si HDMS or Agilent G6224A spectrometer.

The luminescent spectra were measured at JASCO FP-6500 instrument.

The decay spectra were measured at room temperature with Edinburgh Instruments FLS1000 instrument.

The EPR measurements were performed on a Bruker A200 spectrometer equipped with a high sensitivity cavity (ER4119HS) in conjunction with microwave bridge Bruker A40X.

X-ray photoelectron spectroscopy (XPS) signals were collected on a Thermo ESCALAB Xi+ spectrometer.

UV-vis spectra were measured on an HP 8453 spectrometer.

The photoluminescence quantum yields (ΦPL) of the samples were measured on HAMAMATSU C13534-31 for absolute PL quantum yield.

The light sources are 450 nm LED, which were purchased from the Beijing China Education Au-light Co., Ltd.

X-ray diffraction data were collected using synchrotron radiation and MAR325 CCD detector at Shanghai Synchrotron Radiation BL17B Beamline. The structure was solved

by direct methods and refined on F2 by full-matrix least-squares methods with SHELXTL-2018 version software.[1-3]

1.1 General Procedure for UV-vis and Fluorescence Measurements

The samples (1.0 ×10^{-5} M) in DMSO were taken at UV-vis measurements. The fluorescence experiments were carried out using a liquid of samples (1.0 ×10^{-5} M) in DMSO under anaerobic conditions and excitation wavelength is 405 nm. Photoluminescence decay experiments were obtained with a 450 nm laser with samples (1.0 ×10^{-5} M) in DMSO also under anaerobic conditions.

1.2 General Procedure Photocatalytic Oxidation of C(sp^3)-H Bonds

Typically, substrates (0.01 mmol) and catalysts (5 mol%) were dissolved in acetonitrile (2 mL) with a 10.0 mL quartz test tube. The reaction was carried out at ambient temperature with O_2 bubbling under illumination with a 450 nm LED and magnetic stirring.

1.3 EPR detection for verify the generation of $^1O_2$ and $O_2^{\bullet-}$

EPR analysis was performed to verify the generation of $^1O_2$ and $O_2^{\bullet-}$ under light irradiation by using 5,5-dimethyl-1-pyrroline-N-oxide (DMPO) and 2,2,6,6-tetramethyl-piperidine (TEMP) as the spin trapping agents, respectively. EPR signals were obtained with a mixture (400 μL) of the spin trapping agent (0.1 M) and cage (1.0 mM) and added to the EPR tube on irradiation under an oxygen atmosphere.

1.4 Electrochemical measurement

All electrochemical tests were performed on CHI 660E Electrochemical Workstation with a conventional three-electrode system. The measurements were tested with a scan rate of 100 mV·s^{-1} at room temperature after degassed with nitrogen for 5 minutes. Cyclic voltammetry (CV) was conducted in CH_3CN solution containing 0.1 M *n*-Bu_4NPF_6 electrolyte, using a freshly polished glassy carbon electrode with a diameter of 5 mm as a working electrode, a platinum wire with 0.5 mm diameter as a counter electrode and an Ag/AgCl (3 M KCl) electrode. Ferrocene (Fc) was added as an internal reference after every experiment.

2. Syntheses and characterizations

2.1 Synthesis and characterizations of 1

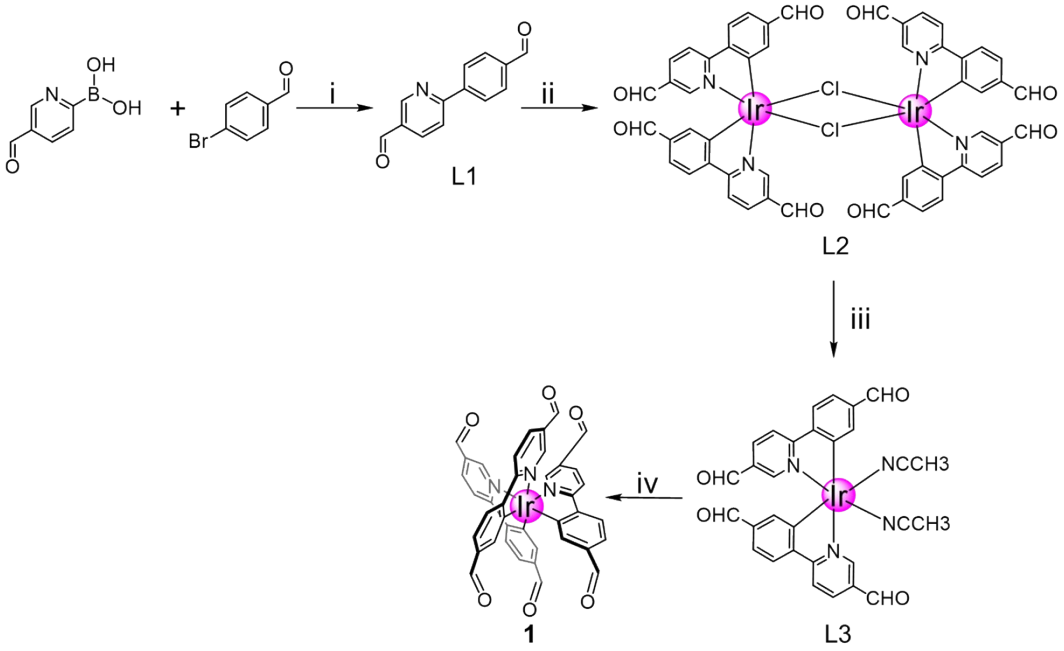

Scheme S1. Synthesis of **1**. Reaction conditions: i) dioxane: water = 4:1 (v/v), 90 °C, Ar, 12 h; ii) $IrCl_3$, 2-methoxyethanol: water =3: 1 (v/v), 120 °C, Ar, 12 h; iii) AgOTf, dry CH_3CN, 60 °C, 2 h; iv) L1, *o*-dichlorobenzene, 180 °C, Ar, 2 h.

6-(4-Formylphenyl)-3-pyridinecarboxaldehyde (L1). 4-Formylphenylboronic acid (1.0 g, 6.7 mmol), 6-bromo-3-pyridinecarboxaldehyde (1.2 g, 6.45 mmol), sodium carbonate (1.9 g, 17.9 mmol), and tetrakis(triphenylphosphine)-palladium (0.30 g, 0.26 mmol) were dissolved in a degassed mixture of dioxane:water (4:1, 30 mL). The mixture was heated at 90 °C under Ar for 12 h. The resulting reaction mixture was cooled down to room temperature and the product was extracted with CH_2Cl_2. Using saturated sodium hydrogen carbonate solution and brine, the organic phase was washed, followed by drying with Na_2SO_4. Then the organic solvent was filtered and evaporated under vacuum, the residue was purified by silica gel column chromatography (ethyl acetate/petroleum ether = 3:1 v/v) to give compound L1 as a white soild (1.1g, 81%).[4]

^{1}H NMR (400 MHz, $CDCl_3$, ppm): *δ* 10.18 (s, 1H), 10.11 (s, 1H), 9.18 (s, 1H), 8.28 (dd, *J* = 12.2, 5.2 Hz, 3H), 8.01 (dd, *J* = 16.2, 8.3 Hz, 3H).

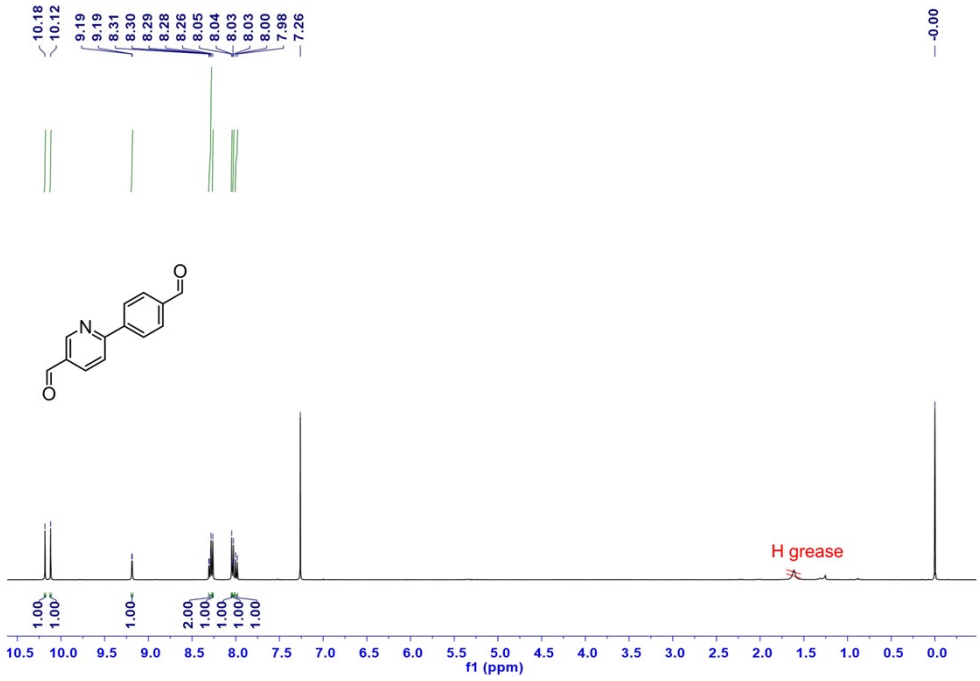

Figure S1. ^{1}H NMR spectrum (400 MHz, $CDCl_3$) of L1.

$[Ir(L1)_2(\mu\text{-}Cl)]_2$ (L2). $IrCl_3$ (0.6 g, 1.7 mmol) was refluxed in a schlenk flask under Ar atmosphere with L1 (0.9 g, 4.25 mmol) in a 3:1 mixture of 2-methoxyethanol and water, and the reaction mixture was stirred for 24 h at 120 °C. The reaction mixture was filtered, washed with water and acetone. The blood red solids were collected and dried under vacuum to give the product L2 (0.72 g, yield 64%).

^{1}H NMR (400 MHz, CD_2Cl_2, ppm): *δ* 9.70 (s, 1H), 9.64 (s, 1H), 9.55 (s, 1H), 8.28 (t, *J* = 7.2 Hz, 2H), 7.88 (d, *J* = 8.1 Hz, 1H), 7.40 (d, *J* = 7.9 Hz, 1H), 6.31 (s, 1H).

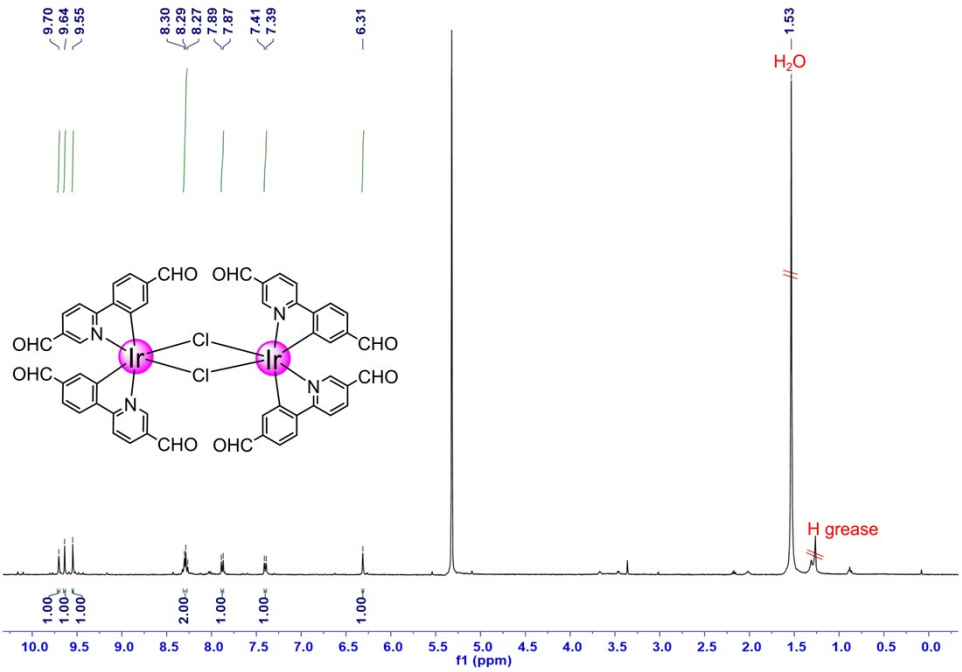

Figure S2. ^{1}H NMR spectrum (400 MHz, CD_2Cl_2) of L2.

[Ir(L1)$_2$(NCCH$_3$)$_2$]OTf (L3). Compound L2 (0.33 g, 0.25 mmol) in 30 mL of dry acetonitrile was heated to dissolve the chloro-bridged dimer at 90 °C keep in dark for 1 h. A 10 mL acetonitrile solution of AgOTf (0.13 g, 0.5 mmol) was added to the solution. The mixture was kept at 60 °C in the dark for 2 h resulted in a gray precipitate. The gray AgCl precipitate was filtered over a Celite pad resulted an orange solution. The solution was concentrated in vacuo, then redissolved in a minimal amount of acetonitrile and precipitating with diethyl ether. The orange yellow crystal precipitates were collected and dried under vacuum to give the product L3 (0.25 g, yield 73%).

^{1}H NMR (400 MHz, CD$_3$CN, ppm): *δ* 9.53 (s, 1H), 8.93 (s, 1H), 8.83 (d, *J* = 1.8 Hz, 1H), 7.85 (dd, *J* = 8.5, 1.9 Hz, 1H), 7.68 (d, *J* = 8.5 Hz, 1H), 7.26 (d, *J* = 8.1 Hz, 1H), 6.74 (dd, *J* = 8.0, 1.6 Hz, 1H), 5.90 (d, *J* = 1.6 Hz, 1H), 1.24 (s, 3H).

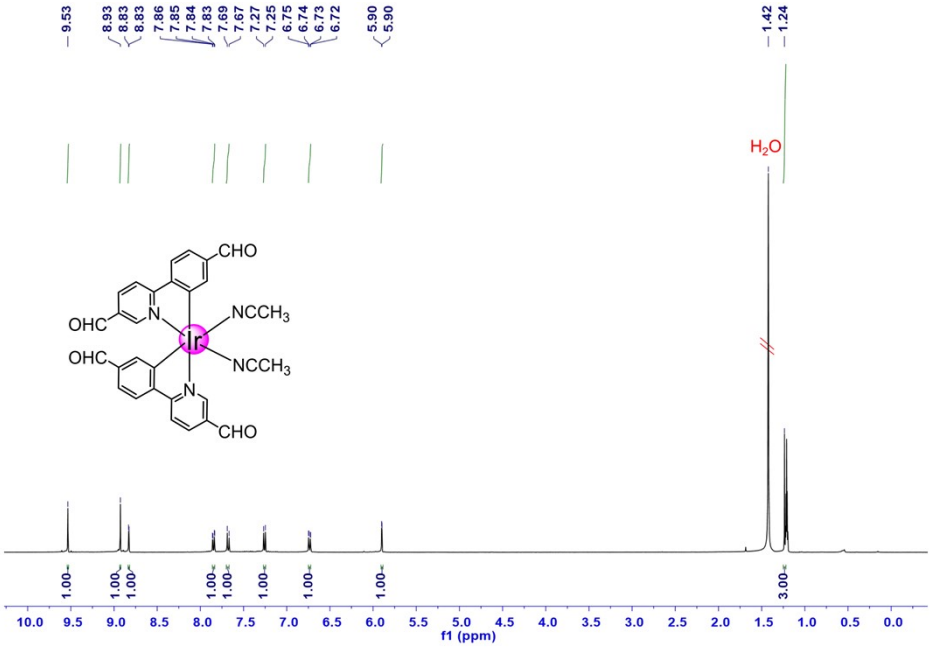

Figure S3. ^{1}H NMR spectrum (400 MHz, CD$_3$CN) of L3.

***fac*-Ir-2CHO (1).** Compound L3 (0.25 g, 0.36 mmol) and L1 (0.076 g, 0.36 mmol) were combined in 18 mL of o-dichlorobenzene and heated at 180 °C under Ar atmosphere for 2 h. After cooling to room temperature, the reaction solution was chromatographed on a silica gel column packed with petroleum ether to first elute o-dichlorobenzene. Switching to dichloromethane, then dichloromethane/ethyl acetate (20:1, v/v) eluted the product, obtained the dark red solids of **1** in 20% yield of 60 mg.

^{1}H NMR (400 MHz, CD_2Cl_2, ppm): δ 9.80 (s, 1H), 9.68 (s, 1H), 8.24 (dd, J = 6.4, 1.4 Hz, 2H), 8.06 (dd, J = 1.9, 0.9 Hz, 1H), 7.98 (d, J = 8.2 Hz, 1H), 7.51 (dd, J = 8.1, 1.7 Hz, 1H), 7.16 (d, J = 1.7 Hz, 1H).

^{13}C NMR (100 MHz, CD_2Cl_2, ppm): δ 193.78, 188.85, 170.15, 161.52, 150.45, 148.65, 139.90, 138.23, 131.73, 127.18, 121.92, 121.36.

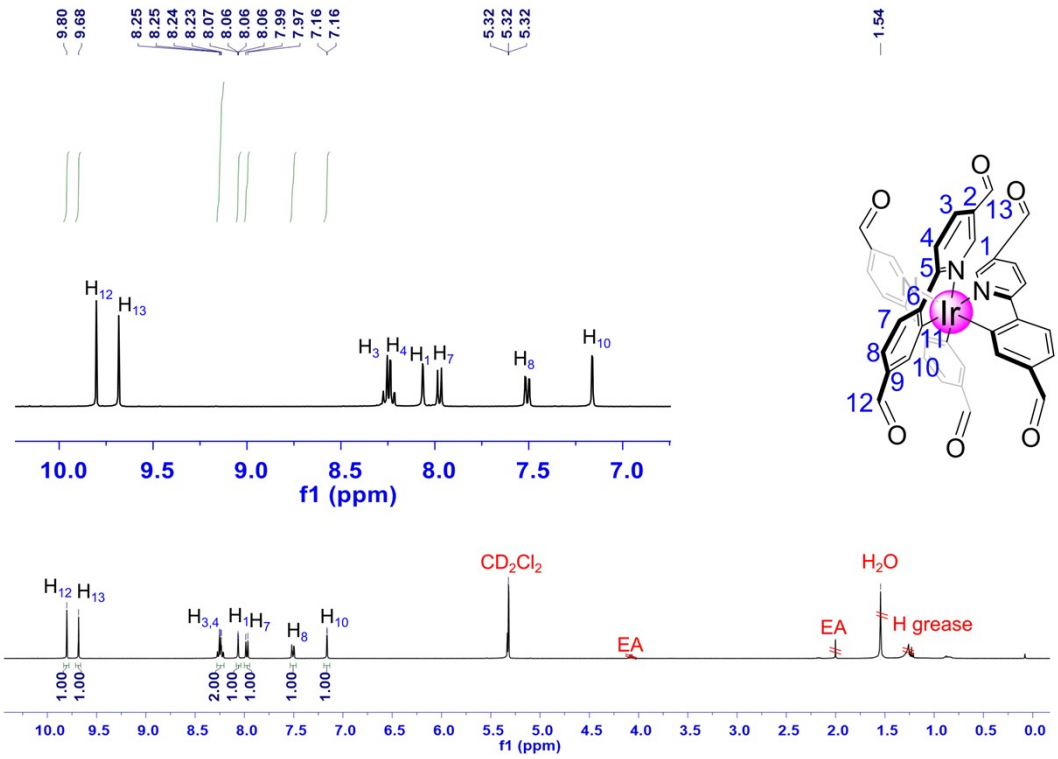

Figure S4. ^{1}H NMR spectra (400 MHz, CD_2Cl_2) of **1**.

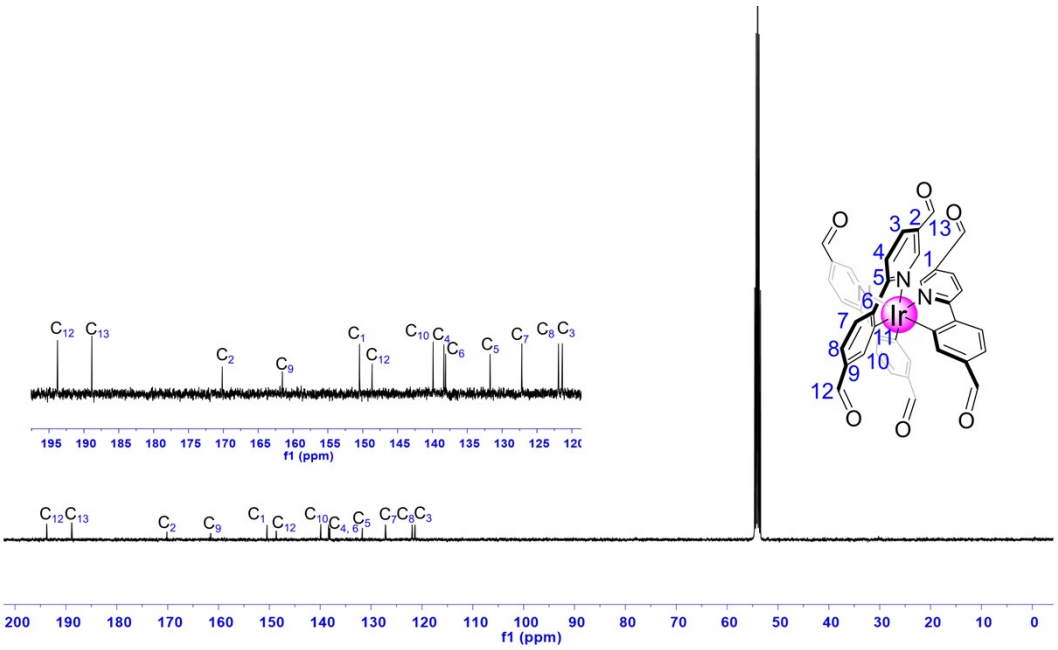

Figure S5. ^{13}C NMR spectra (100 MHz, CD_2Cl_2) of **1**.

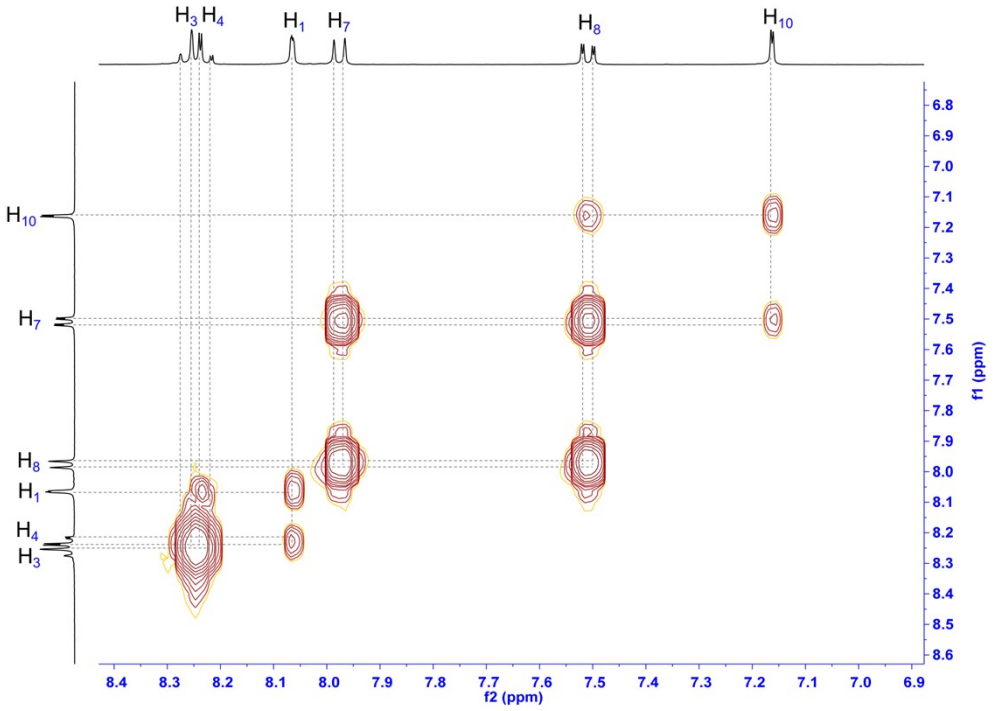

Figure S6. Partial ^{1}H-^{1}H COSY spectra (400 MHz, CD_2Cl_2) of **1**.

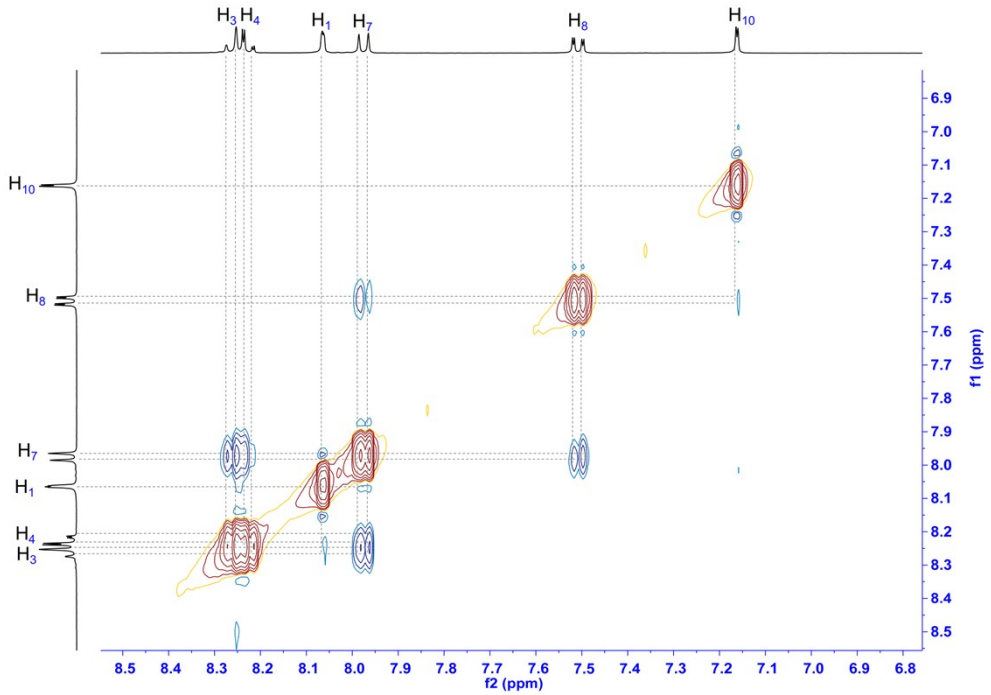

Figure S7. Partial ^{1}H-^{1}H NOE spectra (400 MHz, CD_2Cl_2) of **1**.

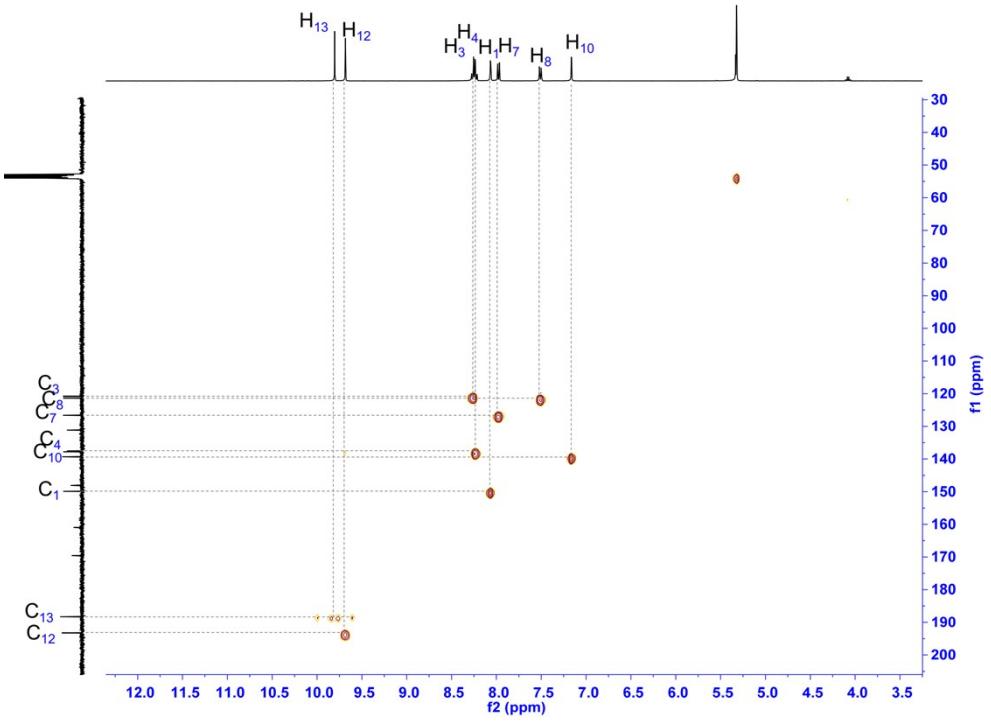

Figure S8. ^{1}H-^{13}C HSQC spectra (400 MHz, CD_2Cl_2) of **1**.

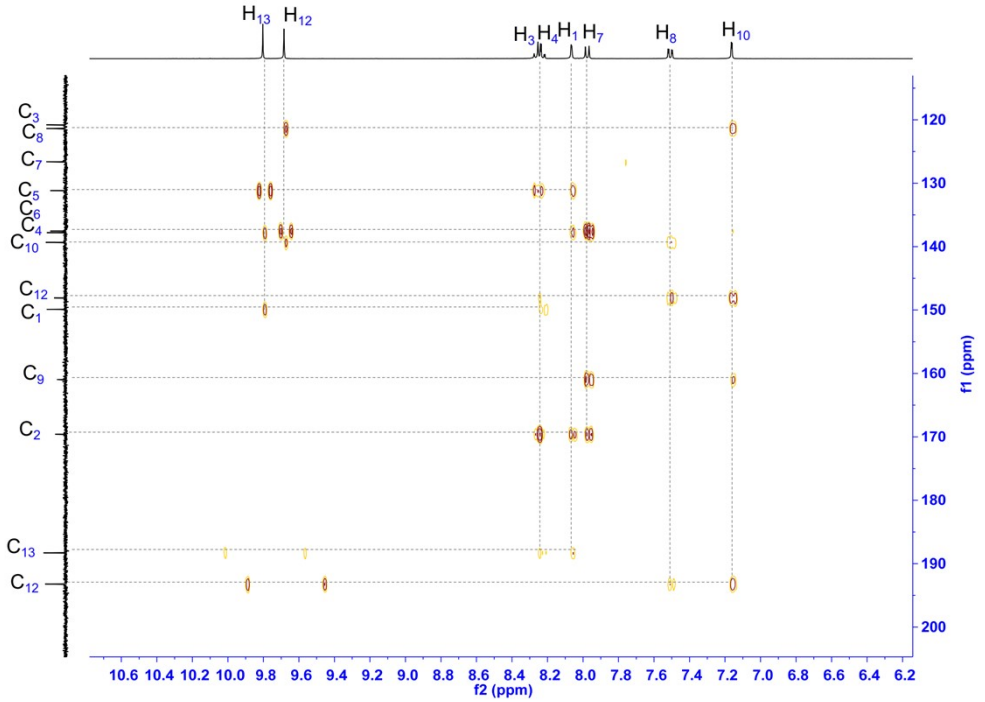

Figure S9. ^{1}H-^{13}C HMBC spectra (400 MHz, CD_2Cl_2) of **1**.

2.2 Synthesis and characterizations of cage 2.

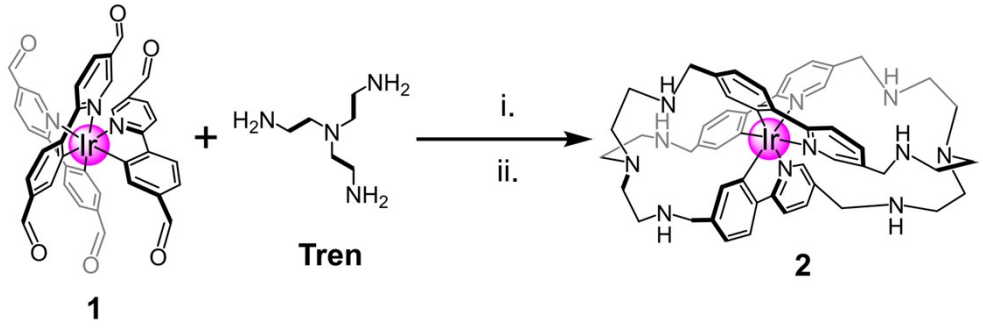

Scheme S2. Synthesis of cage **2**. Reaction conditions: i) CH_3OH/CH_2Cl_2= 1: 1(v/v), Ar, RT, 24 h; ii) $NaBH_4$, RT, 12 h.

Cage **2.** Compound **1** (20 mg, 0.024 mmol, 1.0 equiv.) was dissolved in a CH_3OH/CH_2Cl_2 mixture (1:1 v/v, 20 mL) under argon atmosphere. Following, a 10 mL CH_3OH solution of Tris(2-aminoethyl)amine (**Tren**) (7.2 μL, 0.048 mmol, 2.0 equiv.) was added dropwise using a dropping funnel, then glacial acetic acid (5 mol%) was added. The resulting solution was vigorously stirred at room temperature for 24 h. After reacted over, the bright red solution was reserved without further processing. Then, sodium borohydride (18 mg, 0.48 mmol) was added in five batches at ice-water bath, and the reaction was

stirred for a further 12 h at room temperature. Water (10 mL) was then added, and the reaction stirred for a further 2 hours. The mixture was extracted with CH_2Cl_2 and the organic layer dried over Na_2SO_4, filtered, and evaporated, resulting light yellow solid was dissolved in of the mixture of CH_3OH/CH_2Cl_2 and transferred into glass tubes. Diethyl ether was diffused into the mixture solution and got the yellow crystals of cage **2** (21 mg, yield 84%) after about two weeks.

^{1}H NMR (400 MHz, DMSO-*d*$_6$, ppm): δ 8.02 (d, J = 8.4 Hz, 1H), 7.77 – 7.63 (m, 2H), 7.14 (d, J = 2.0 Hz, 1H), 6.84 (dd, J = 8.0, 1.8 Hz, 1H), 6.77 (d, J = 1.7 Hz, 1H), 4.85 (s, 1H, NH), 4.21 (d, J = 5.3 Hz, 1H), 4.16 (d, J = 5.1 Hz, 1H), 3.46 (d, J = 11.5 Hz, 1H), 3.24 (d, J = 11.4 Hz, 1H), 2.58 (s, 1H), 2.48 – 2.35 (m, 3H), 1.60 (s, 1H, NH').

^{13}C NMR (100 MHz, DMSO-*d*$_6$, ppm): δ 165.09, 160.13, 146.20, 143.03, 138.09, 135.49, 124.37, 119.17, 64.04, 53.91, 51.80, 48.14.

MALDI-TOF-MS: m/z [**3**+Na]$^+$ calcd for $C_{51}H_{60}IrN_{11}Na$: 1042.4555, found: 1042.4530.

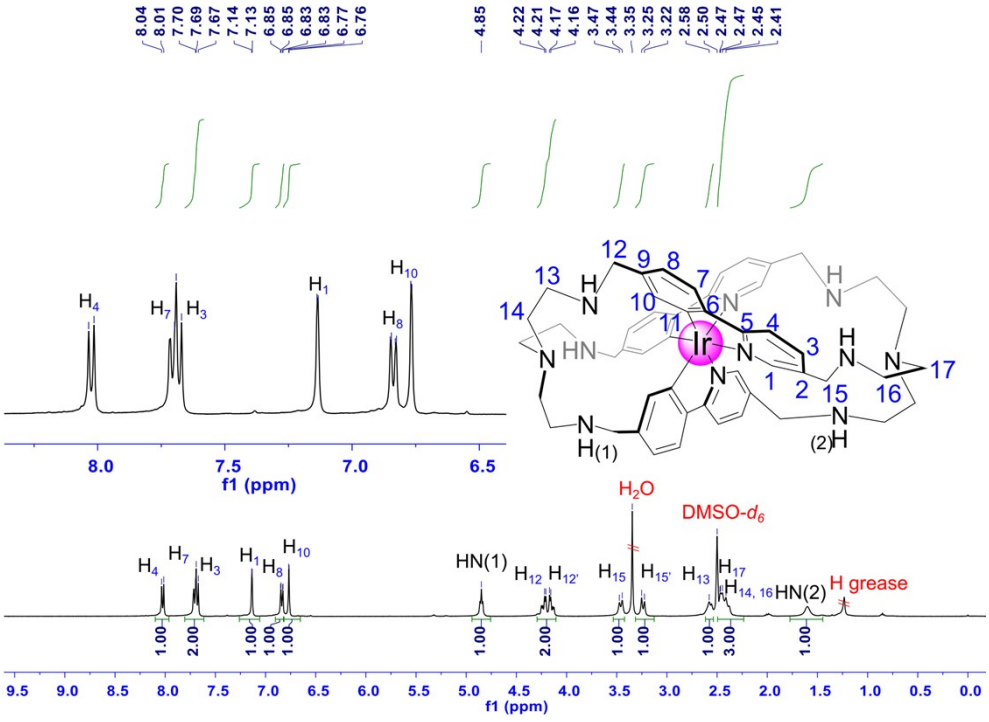

Figure S10. ^{1}H NMR spectra (400 MHz, DMSO-d_6) of cage **2**.

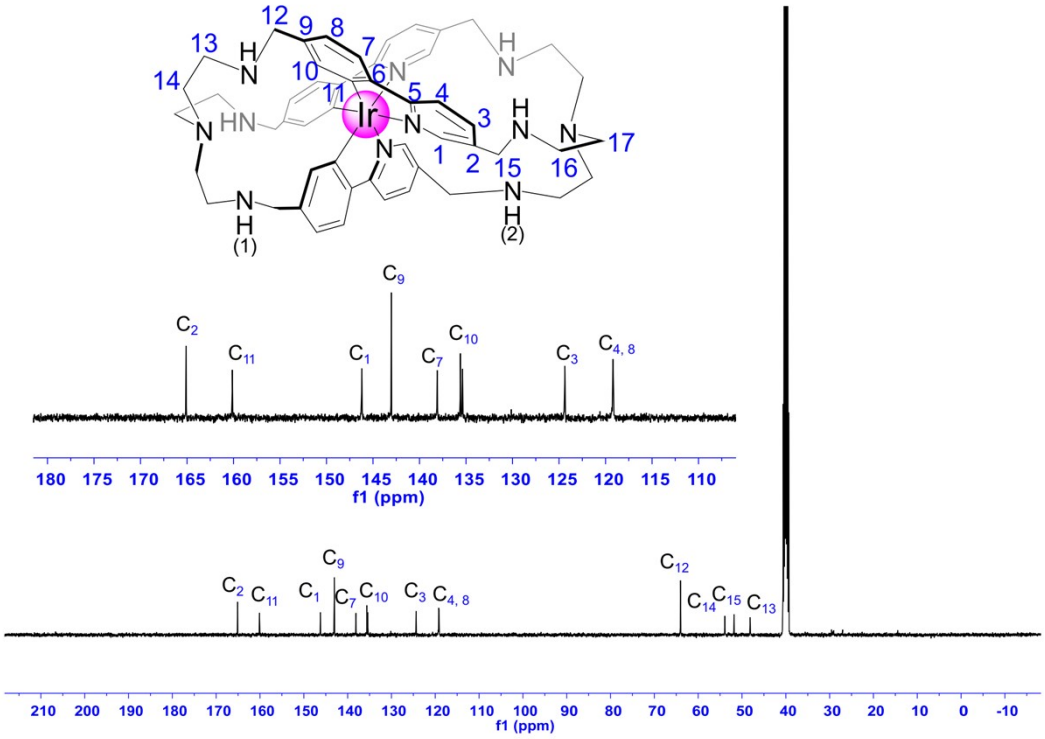

Figure S11. ^{13}C NMR spectra (100 MHz, DMSO-d_6) of cage **2**.

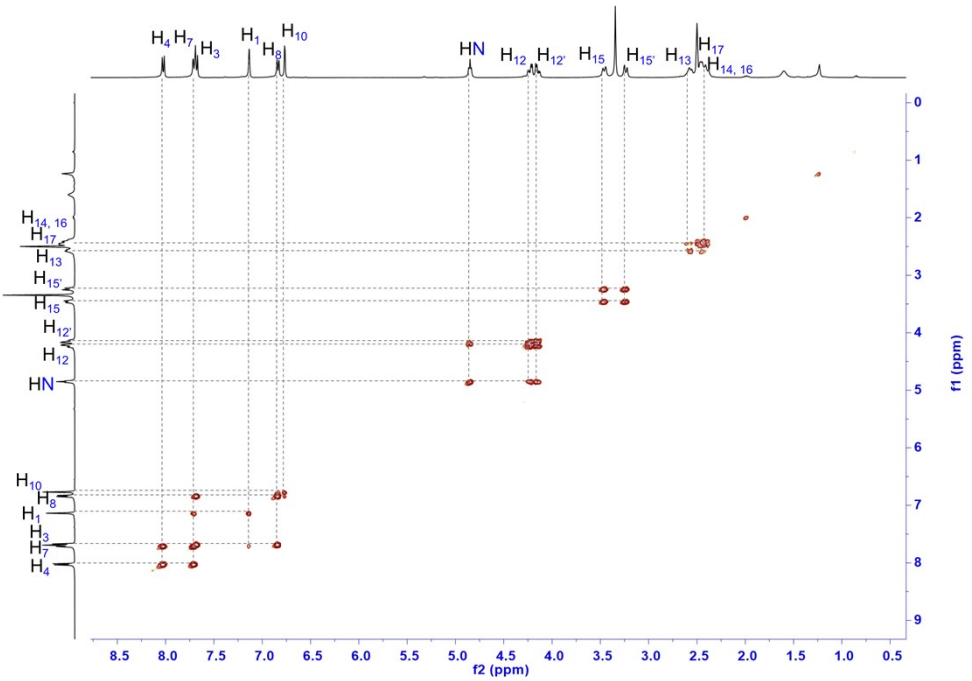

Figure S12. ^{1}H-^{1}H COSY spectra (400 MHz, DMSO-d_6) of cage **2**.

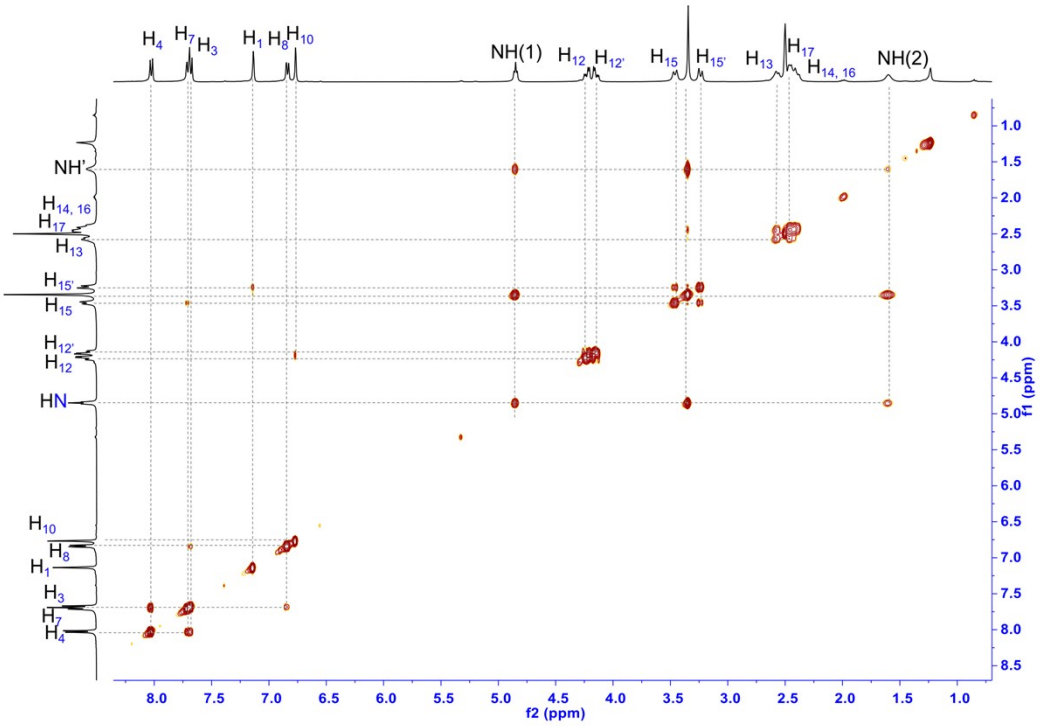

Figure S13. ^{1}H-^{1}H NOE spectra (400 MHz, DMSO-d_6) of **2**.

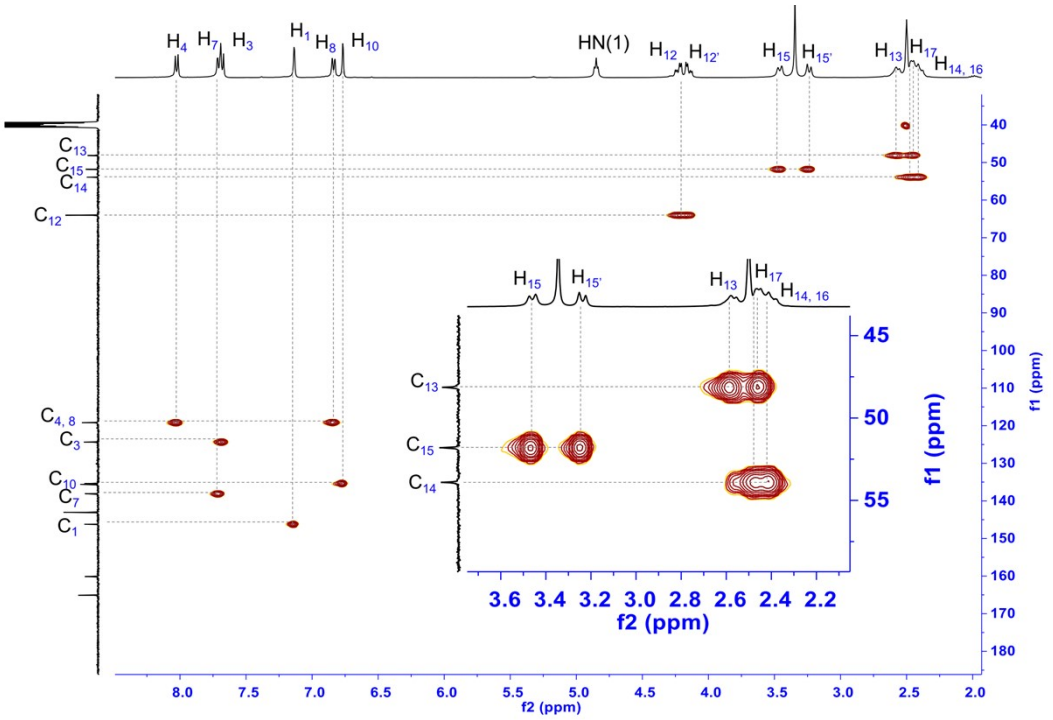

Figure S14. ^{1}H-^{13}C HSQC spectra (400 MHz, DMSO-d_6) of **2**.

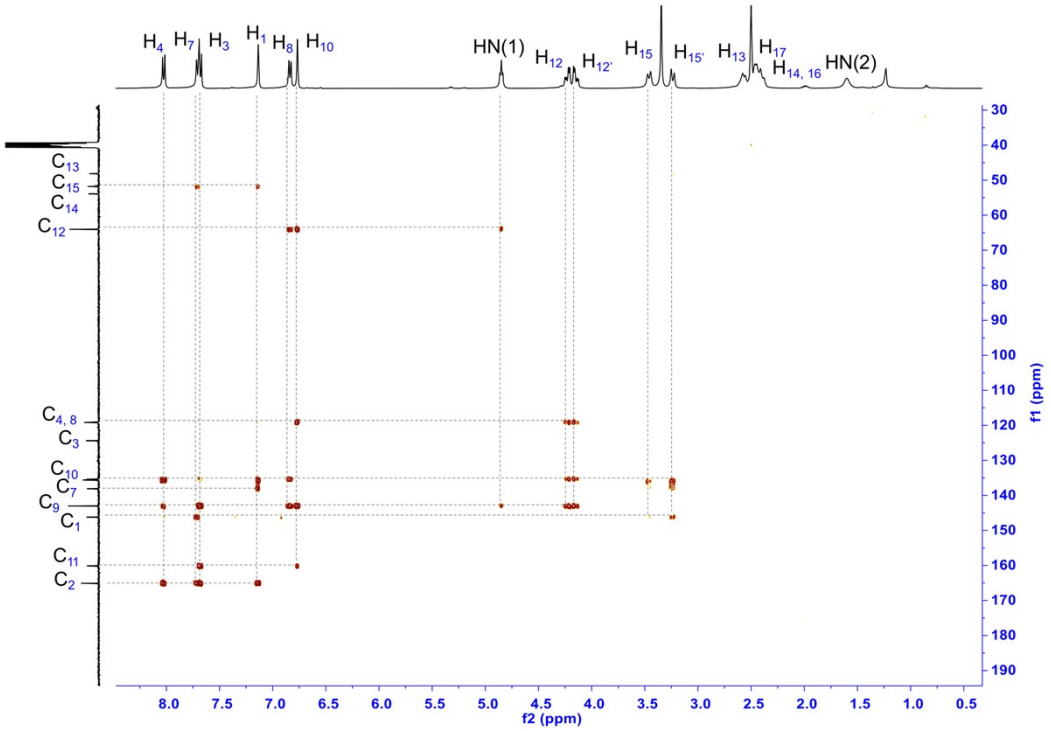

Figure S15. ^{1}H-^{13}C HMBC spectra (400 MHz, DMSO-d_6) of **2**.

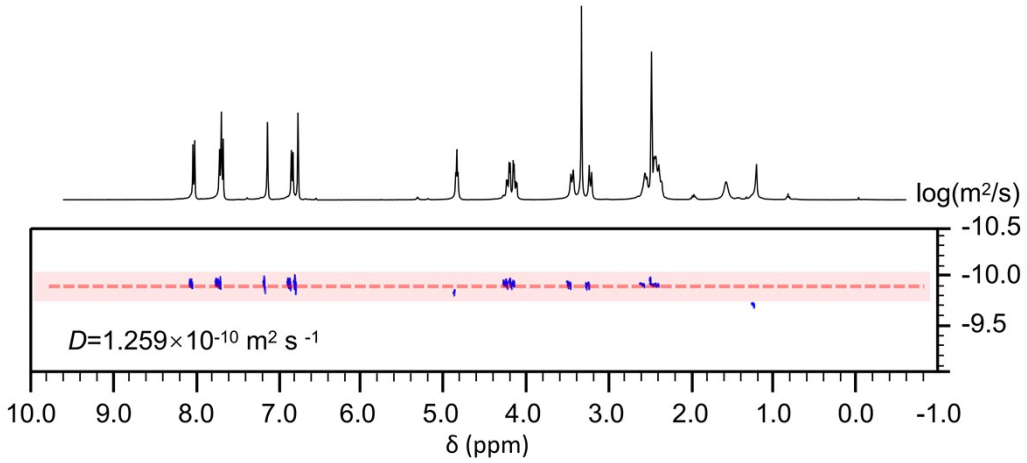

Figure S16. ^{1}H DOSY spectra (400 MHz, DMSO-d_6) of **2**. The insert shows the diffusion coefficient (D) value of **2**.

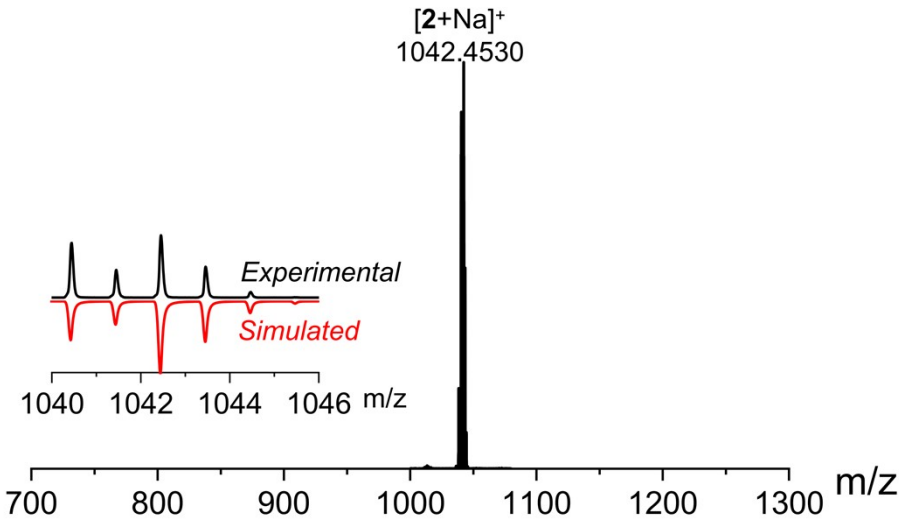

Figure S17. MALDI-TOF-MS spectra of cage **2** in methanol solution. The inserts show the measured and simulated isotopic patterns.

Species Assigned	Caculated Value	Measured Value
[**2**+Na]$^+$	1042.4555	1042.4530

2.3 Synthesis and characterizations of cage Cu_2@2.

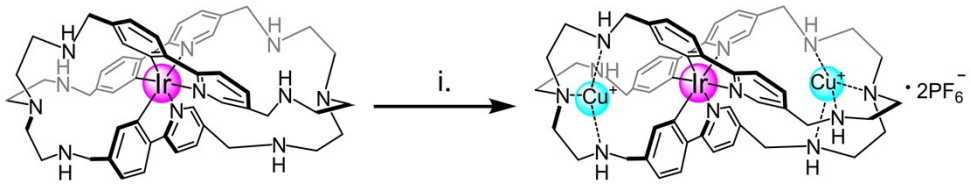

Scheme S3. Synthesis of **Cu_2@2**. Reaction conditions: i) $Cu(CH_3CN)_4 \cdot PF_6$, dry CH_3CN, Ar, RT, 24 h.

Cu_2@2. 15.3 mg (0.015 mmol, 1.0 equiv.) of cage **2** was dissolved in 2 mL acetonitrile. $[Cu(MeCN)_4]PF_6$ (12.3 mg, 0.033 mmol, 2.2 equiv.) were added into the solution argon atmosphere. The yellow solution turned to pale orange. The mixture was further stirred for 3 h before filtrated. Added 0.5 mL CH_2Cl_2 in the filtrate and transferred into a tube, and then diethyl ether was diffused into the mixture solution. After about two weeks, 16 mg (yield 83%) yellow crystals were grown on the glass wall.

^{1}H NMR (400 MHz, DMSO-d_6, ppm): δ 8.05 (d, J = 8.2 Hz, 1H), 7.81 (dd, J = 8.3, 2.0 Hz, 1H), 7.74 (d, J = 2.0 Hz, 1H), 7.61 (d, J = 7.8 Hz, 1H), 7.51 (d, J = 1.8 Hz, 1H), 6.76 (dd, J = 7.9, 1.7 Hz, 1H), 4.46 (t, J = 12.0 Hz, 1H), 3.98 (d, J = 12.4 Hz, 1H), 3.72 (d, J = 10.3 Hz, 1H), 3.56 - 3.46 (m, 1H), 3.43 (d, J = 11.1 Hz, 2H), 3.33 (s, 1H), 2.90 (q, J = 11.3 Hz, 2H), 2.76 (d, J = 11.8 Hz, 3H), 2.68 (d, J = 14.1 Hz, 3H).

^{13}C NMR (100 MHz, DMSO-d_6, ppm): δ 165.54, 159.25, 147.31, 143.71, 139.68, 138.96, 133.91, 124.01, 121.32, 119.34, 57.06, 53.18, 51.21, 50.07.

ESI-TOF-MS: m/z [**Cu_2@2**]$^{2+}$ calcd for $C_{51}H_{60}Cu_2IrN_{11}$: 572.6616, found: 572.6611; [**Cu_2@2**+PF_6^-]$^+$ calcd for $C_{51}H_{61}Cu_2IrN_{11}PF_6$: 1290.2880, found: 1290.2891.

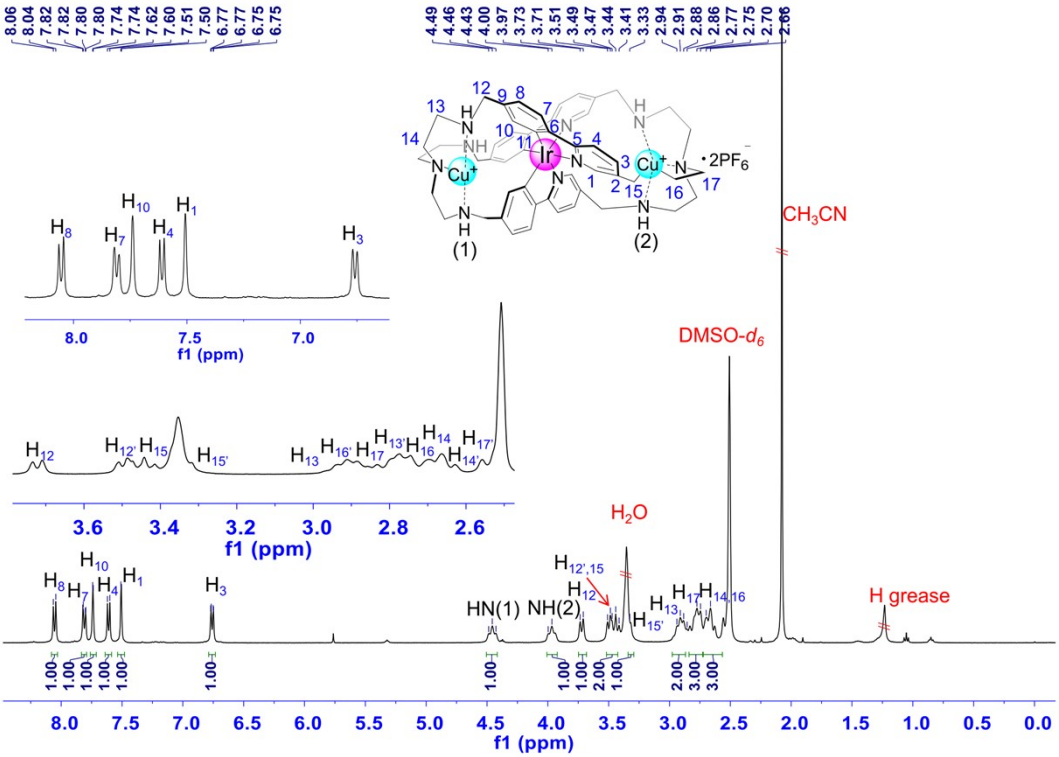

Figure S18. ^{1}H NMR spectra (400 MHz, DMSO-d_6) of **Cu_2@2**.

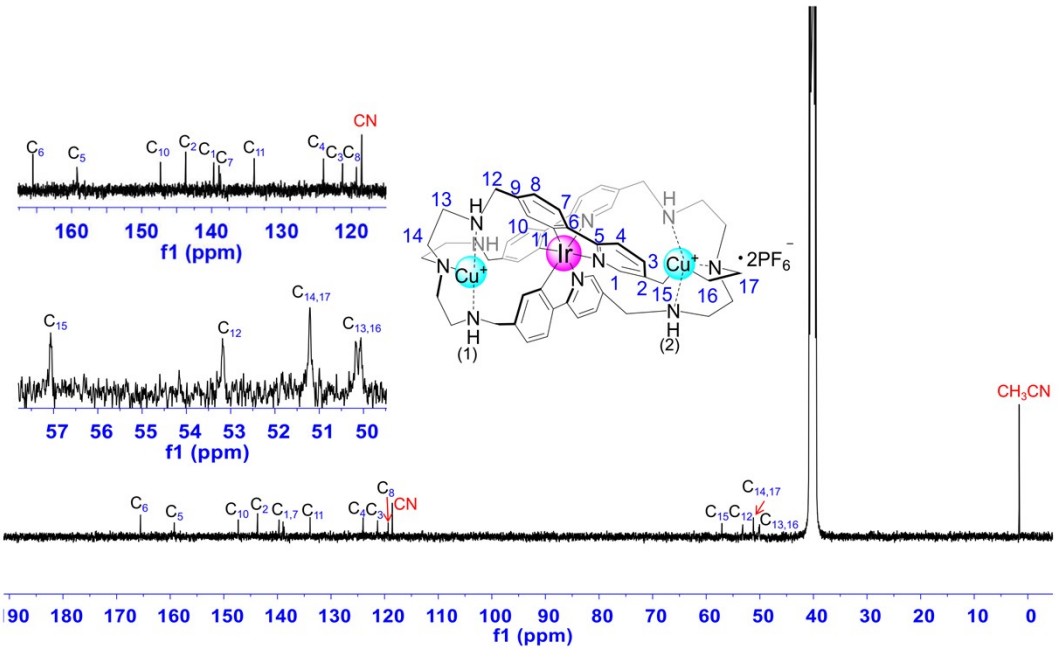

Figure S19. ^{13}C NMR spectra (100 MHz, DMSO-d_6) of **Cu_2@2**.

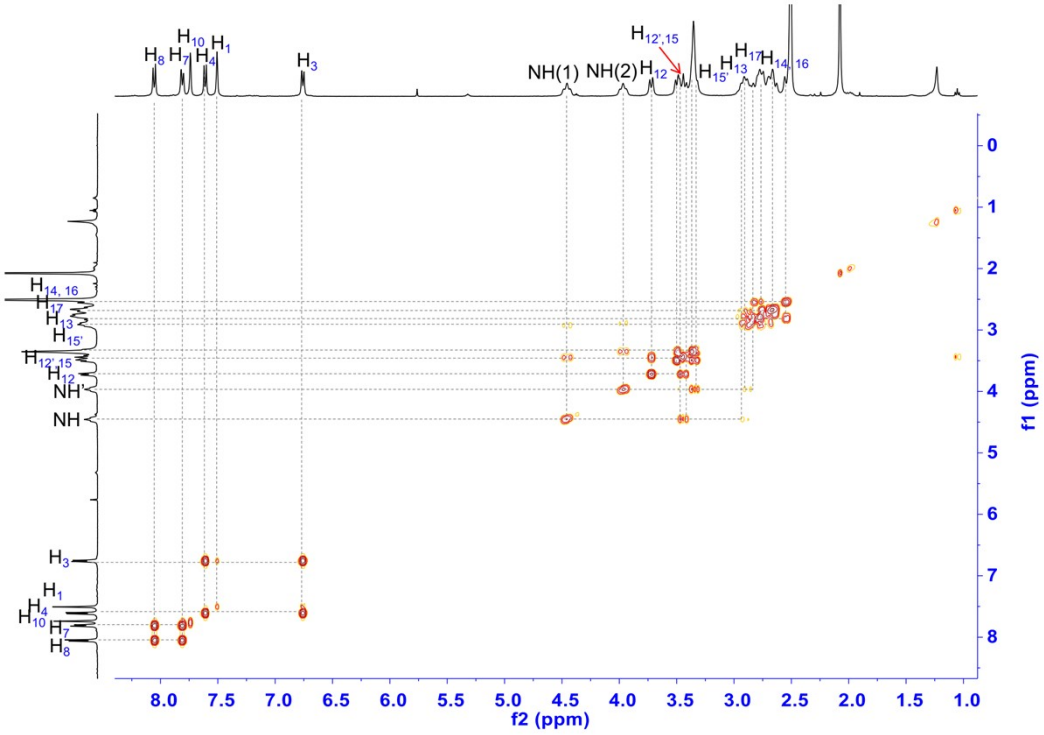

Figure S20. ^{1}H-^{1}H COSY spectra (400 MHz, DMSO-d_6) of **Cu_2@2**.

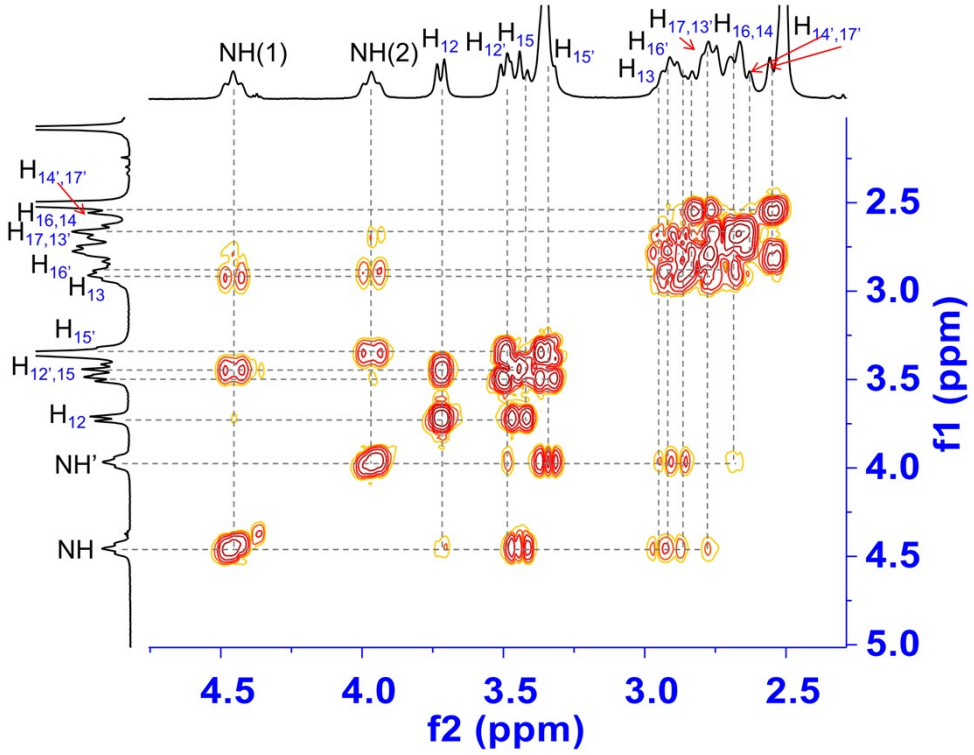

Figure S21. Partial ^{1}H-^{1}H COSY spectra (400 MHz, DMSO-d_6) of **Cu_2@2**.

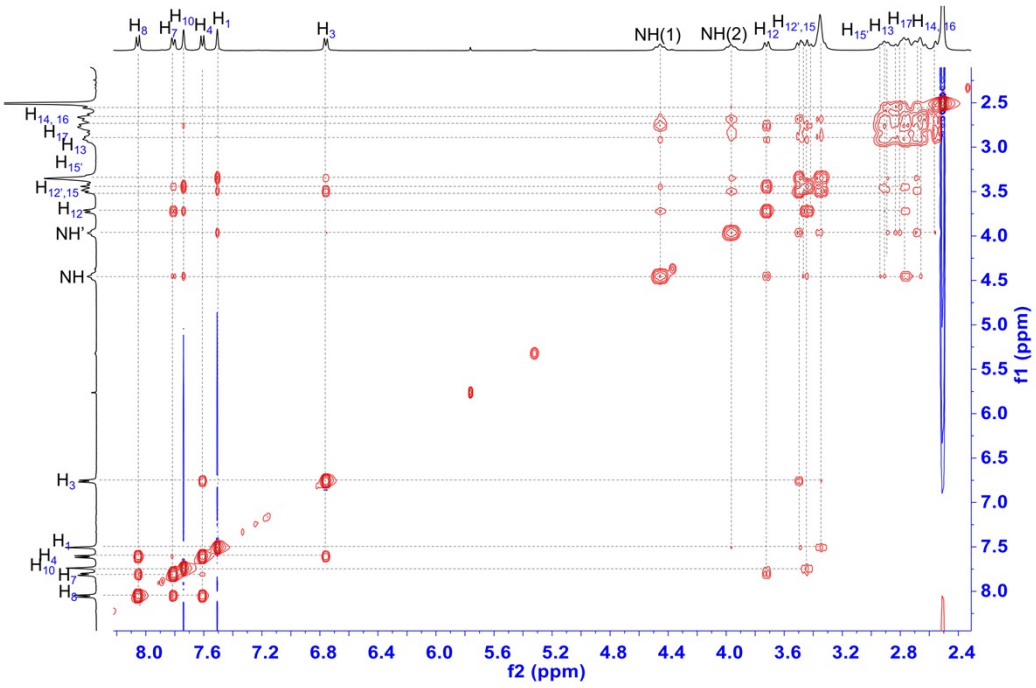

Figure S22. ^{1}H-^{1}H NOE spectra (400 MHz, DMSO-d_6) of **Cu_2@2**.

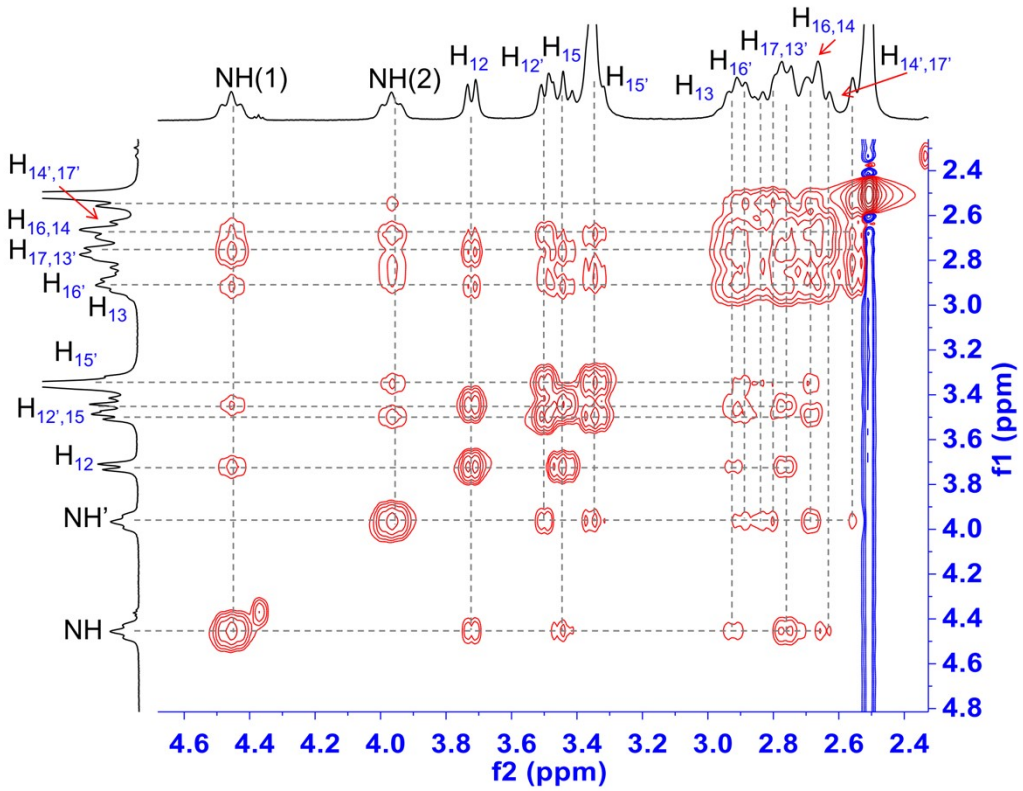

Figure S23. Partial ^{1}H-^{1}H NOE spectra (400 MHz, DMSO-d_6) of **Cu_2@2**.

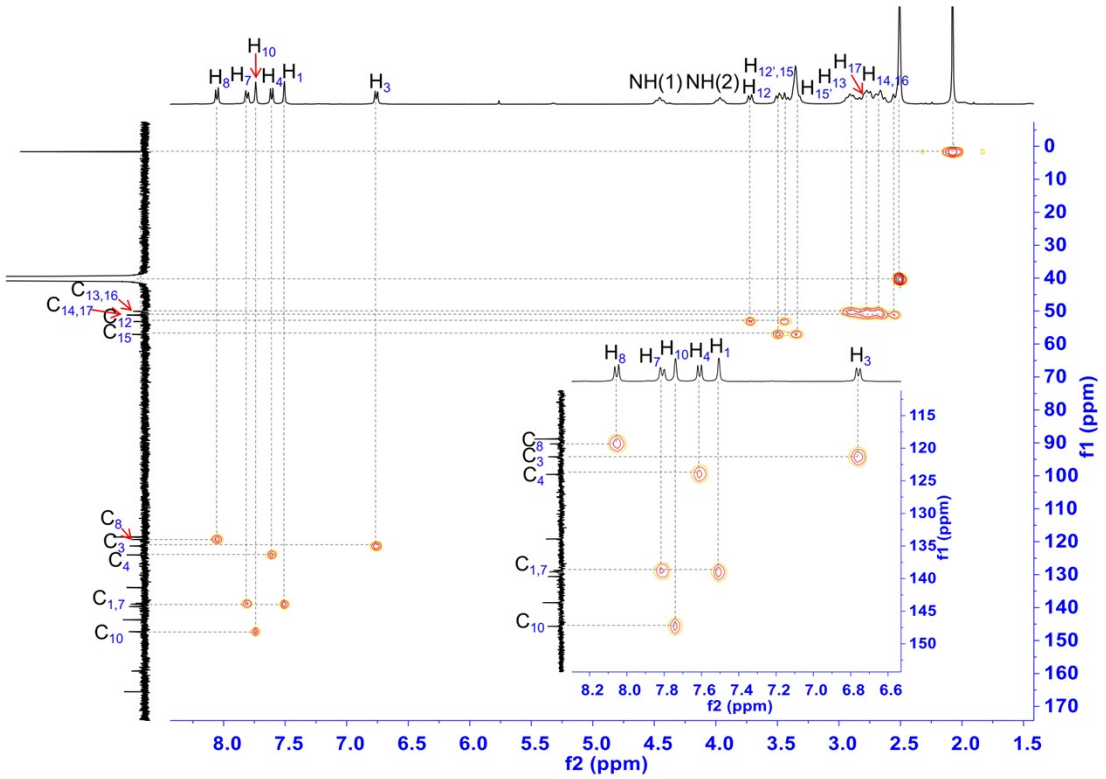

Figure S24. ^{1}H-^{13}C HSQC spectra (400 MHz, DMSO-d_6) of **Cu_2@2**.

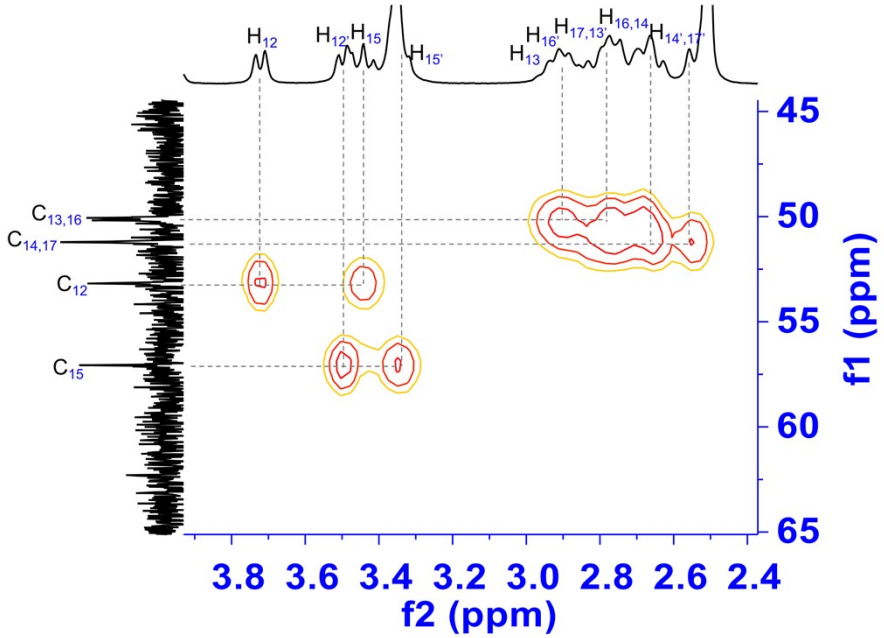

Figure S25. Partial ^{1}H-^{13}C HSQC spectra (400 MHz, DMSO-d_6) of **Cu_2@2**.

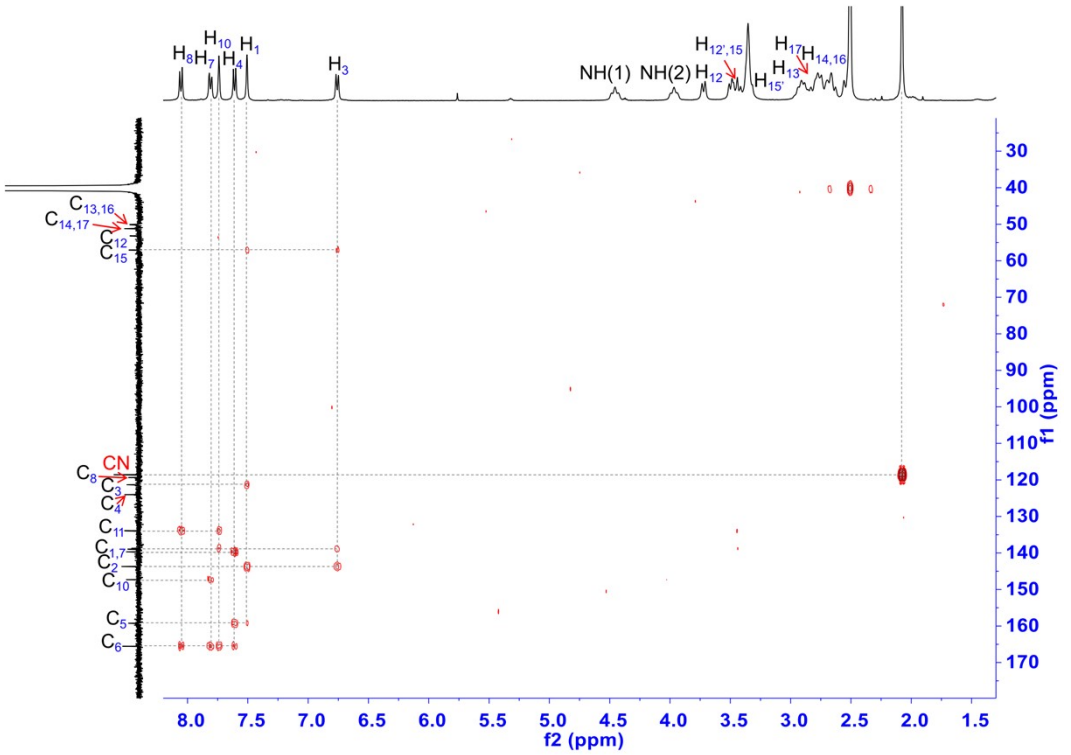

Figure S26. ^{1}H-^{13}C HMBC spectra (400 MHz, DMSO-d_6) of **Cu_2@2**.

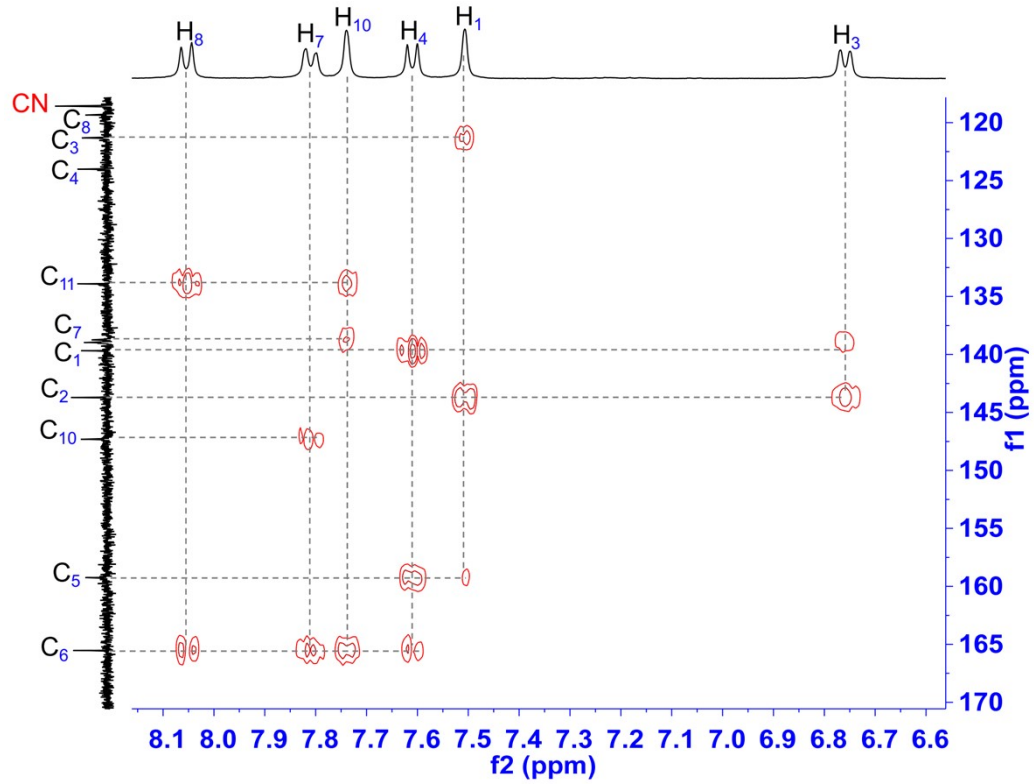

Figure S27. Partial ^{1}H-^{13}C HMBC spectra (400 MHz, DMSO-d_6) of **Cu_2@2**.

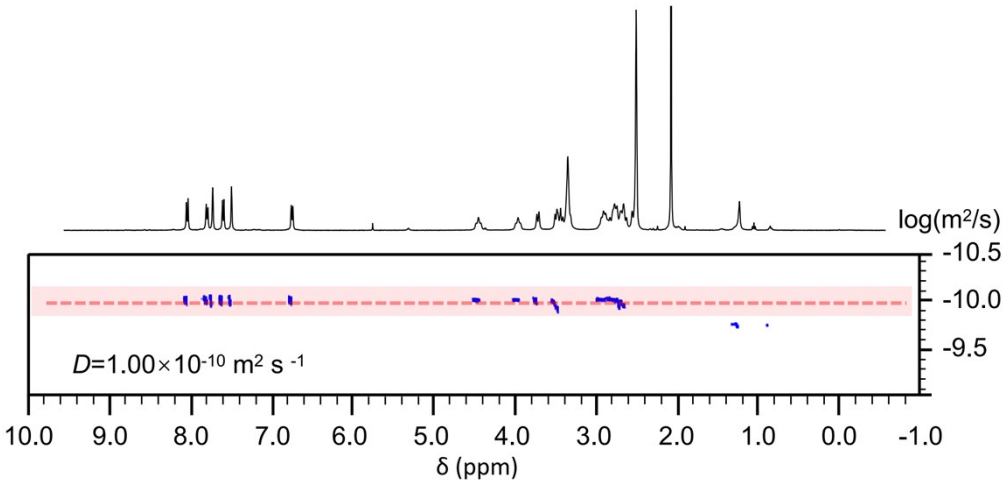

Figure S28. ^{1}H DOSY spectra (400 MHz, DMSO-d_6) of **Cu_2@2**. The insert shows the diffusion coefficient (D) value of **Cu_2@2**.

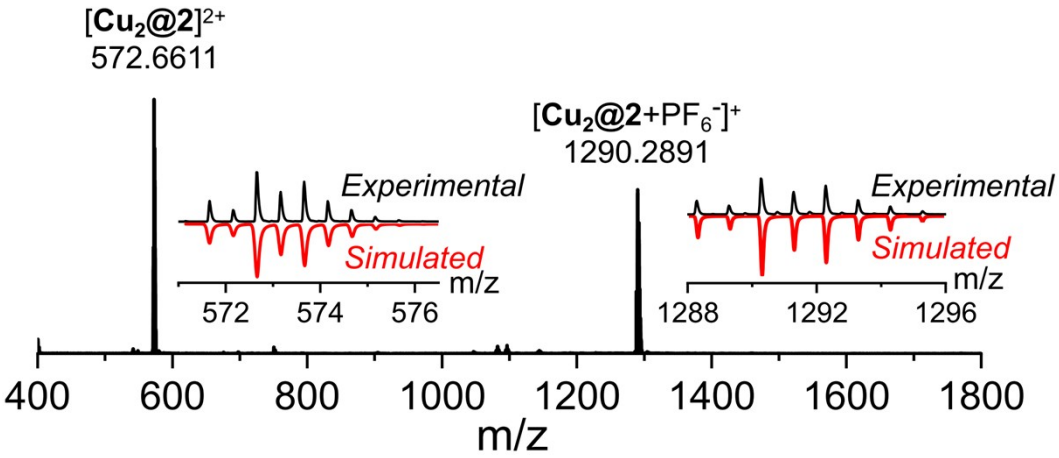

Figure S29. ESI-TOF-MS spectra of **Cu_2@2** in methanol solution. The inserts show the measured and simulated isotopic patterns.

Species Assigned	Caculated Value	Measured Value
[**Cu_2@2**]$^{2+}$	572.6616	572.6611
[**Cu_2@2**+PF_6^-]$^{+}$	1290.2880	1290.2891

3. Crystallography

Table S1. Crystal data for ligand **1** (CCDC **NO. 2376260**).

Molecular formula	$C_{39}H_{24}IrN_3O_6 \cdot CH_3OH$	
Molecular weight	859.36	
Temperature	220(2) K	
Wavelength	0.71073 Å	
Crystal system	Monoclinic	
Space group	P2(1)/n	
Unit cell parameters	*a* = 10.9367(13) Å	α = 90°
	b = 19.534(2) Å	β = 98.291(3)°
	c = 15.6288(16) Å	γ = 90°
	V =3304.0(6) Å^3	
Z	4	
F(000)	1698	
Density (calcd)	1.728 g/cm^3	
Absorption coefficient	4.101 mm^{-1}	
Theta range for data collection	1.679 to 27.526°	
Limiting indices	-14 <= h<= 12, -25 <= k<= 25, -20 <= l<= 15	
Reflections collected	27458	
Independent reflections	7465 [R(int) = 0.1026]	
Completeness to theta = 25.242°	99.5%	
Refinement method	Full-matrix least-squares on F^2	
Data / restraints / parameters	7465 / 1 / 475	
Goodness-of-fit on F^2	0.921	
Final R indices [I>2sigma(I)]	R1 = 0.0559, wR2 = 0.1061	
R indices (all data)	R1 = 0.1137, wR2 = 0.1295	
Largest diff. peak and hole	0.888 and -1.668 e.Å^{-3}	

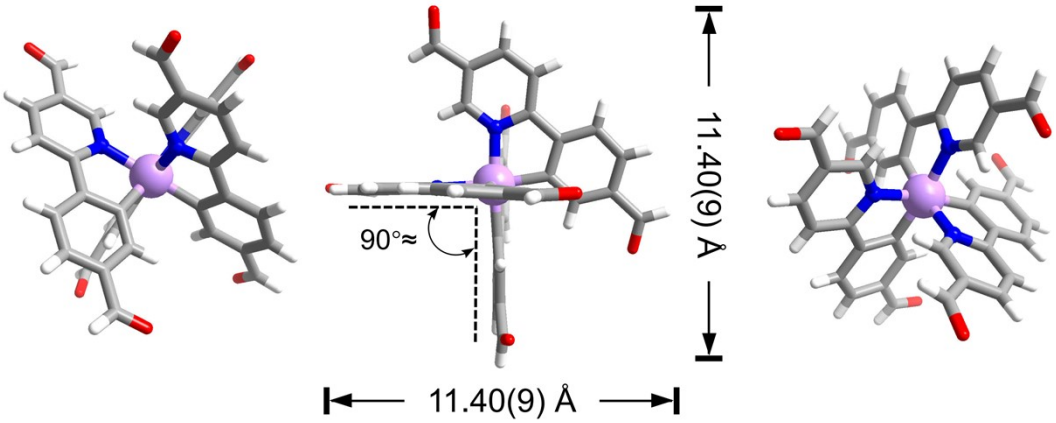

Figure S30. The structure of ligand **1** with octahedron hexa-coordinated configuration, shows the size of single molecular and in different perspective ball-and-stick models.

Ligand **1** was constructed by the alternating arrangement of three ppy ligands on the axial direction of the octahedron defined by Ir(III) ion. The separate N–O sites of ppy ligands were hexa-coordinated to metal center and about 90° from each other, the size of **1** is 11.40(9) Å × 11.40(9) Å.

Table S2. Selected bond distances (Å) and angles (°) in **1**.

Bond	Length	Bond	Length
Ir(01)-C(212)	2.044(10)	C(102)-C(104)	1.377(13)
Ir(01)-C(312)	2.062(9)	C(102)-C(103)	1.499(13)
Ir(01)-C(112)	2.073(8)	C(103)-O(10A)	1.17(2)
Ir(01)-N(101)	2.097(8)	C(103)-O(101)	1.29(2)
Ir(01)-N(301)	2.099(7)	C(103)-H(10G)	0.9597
Ir(01)-N(201)	2.113(8)	C(103)-H(10B)	0.9598
N(101)-C(101)	1.376(10)	C(104)-C(105)	1.364(13)
N(101)-C(106)	1.380(10)	C(104)-H(10C)	0.9400
N(301)-C(301)	1.362(11)	C(105)-C(106)	1.372(12)
N(301)-C(306)	1.373(11)	C(105)-H(10D)	0.9400
N(201)-C(201)	1.352(11)	C(106)-C(107)	1.479(12)
N(201)-C(206)	1.386(11)	C(107)-C(112)	1.399(12)
Bond	Angle	Bond	Angle
C(212)-Ir(01)-C(312)	95.6(3)	C(312)-Ir(01)-N(201)	173.6(3)
C(212)-Ir(01)-C(112)	95.9(3)	C(112)-Ir(01)-N(201)	91.0(3)
C(312)-Ir(01)-C(112)	93.7(3)	N(101)-Ir(01)-N(201)	94.6(3)
C(212)-Ir(01)-N(101)	172.4(3)	N(301)-Ir(01)-N(201)	95.1(3)
C(312)-Ir(01)-N(101)	90.6(3)	C(101)-N(101)-C(106)	117.9(8)
C(112)-Ir(01)-N(101)	79.2(3)	C(101)-N(101)-Ir(01)	125.9(6)
C(212)-Ir(01)-N(301)	89.1(3)	C(106)-N(101)-Ir(01)	116.2(6)
C(312)-Ir(01)-N(301)	80.5(3)	C(301)-N(301)-C(306)	119.3(8)
C(112)-Ir(01)-N(301)	172.7(3)	C(301)-N(301)-Ir(01)	126.6(6)
N(101)-Ir(01)-N(301)	96.3(3)	C(306)-N(301)-Ir(01)	114.0(6)
C(212)-Ir(01)-N(201)	79.6(3)	C(201)-N(201)-C(206)	119.4(8)
C(201)-N(201)-Ir(01)	126.0(7)	C(102)-C(101)-N(101)	121.6(9)
C(206)-N(201)-Ir(01)	114.7(6)	C(102)-C(101)-H(10A)	119.2

Table S3. Crystal data for cage **2** (CCDC **NO. 2381218**).

Molecular formula	C_{51} H_{60} Ir N_{11}·$C_2H_{10}O_{0.5}$	
Molecular weight	1056.36	
Temperature	299(2) K	
Wavelength	0.71073 Å	
Crystal system	Triclinic	
Space group	*P-1*	
Unit cell parameters	*a* = 23.1792(3) Å	α = 90°
	b = 23.1792(3) Å	β = 90°
	c = 23.1792(3) Å	γ = 90°
	V =12453.6(5) Å^3	
Z	8	
F(000)	5992	
Density (calcd)	1.598 g/cm^3	
Absorption coefficient	6.047 mm^{-1}	
Theta range for data collection	7.148 to 78.475°	
Limiting indices	-29 <= h<= 28, -29 <= k<= 29, -29 <= l<= 29	
Reflections collected	54432	
Independent reflections	4413 [R(int) = 0.0410]	
Completeness to theta = 25.242°	99.0%	
Refinement method	Full-matrix least-squares on F^2	
Data / restraints / parameters	4413 / 1 / 240	
Goodness-of-fit on F^2	0.869	
Final R indices [I>2sigma(I)]	R1 = 0.0392, wR2 = 0.1095	
R indices (all data)	R1 = 0.0400, wR2 = 0.1115	
Largest diff. peak and hole	0.748 and -1.415 e.Å^{-3}	

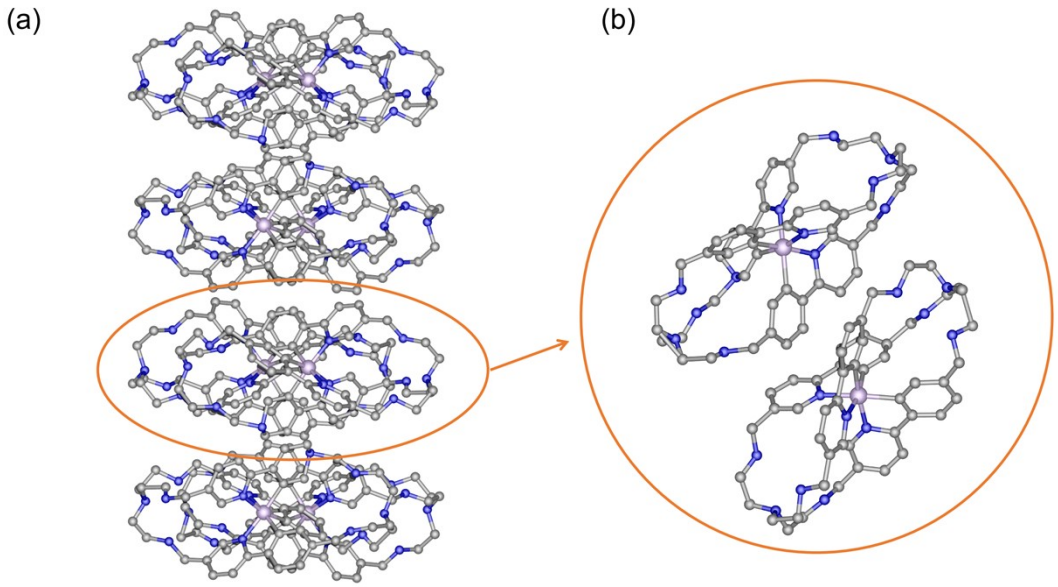

Figure S31. (a) Crystal stacking of **2** in *x-axis* view. (b) Circled part of **2** in *y-axis* view for showing the cage arrangement more clearly. Color code: C, grey; N, blue; Ir, violet. Hydrogen atoms and lattice solvent molecules of diethyl ether are omitted for clarity.

Table S4. Selected bond distances (Å) and angles (°) in **2**.

Bond	Length	Bond	Length
Ir(1)-C(46)	2.022(4)	N(7)-C(28)	1.357(5)
Ir(1)-C(13)	2.020(4)	N(8)-C(19)	1.428(8)
Ir(1)-C(30)	2.024(4)	N(8)-C(18)	1.478(7)
Ir(1)-N(5)	2.127(3)	N(9)-C(51)	1.441(6)
Ir(1)-N(7)	2.130(3)	N(9)-C(52)	1.461(6)
Ir(1)-N(6)	2.135(3)	C(10)-C(11)	1.415(6)
N(1)-C(3)	1.470(13)	C(11)-C(12)	1.431(6)
N(1)-C(1)	1.484(12)	C(12)-C(14)	1.385(6)
N(1)-C(2)	1.500(13)	C(12)-C(13)	1.412(6)
N(5)-C(11)	1.362(5)	C(13)-C(15)	1.413(6)
N(5)-C(8)	1.362(5)	C(14)-C(16)	1.399(7)
N(6)-C(41)	1.356(5)	C(15)-C(17)	1.387(6)
N(6)-C(44)	1.358(5)	C(16)-C(17)	1.376(7)
N(7)-C(25)	1.348(5)	C(17)-C(18)	1.477(7)
Bond	Angle	Bond	Angle
C(46)-Ir(1)-C(13)	94.68(15)	C(30)-Ir(1)-N(6)	165.29(14)
C(46)-Ir(1)-C(30)	90.75(15)	N(5)-Ir(1)-N(6)	92.82(12)
C(13)-Ir(1)-C(30)	94.13(16)	N(7)-Ir(1)-N(6)	90.45(12)
C(46)-Ir(1)-N(5)	169.09(13)	C(3)-N(1)-C(1)	109.2(8)
C(13)-Ir(1)-N(5)	78.91(15)	C(3)-N(1)-C(2)	112.0(9)
C(30)-Ir(1)-N(5)	98.46(14)	C(1)-N(1)-C(2)	104.6(9)
C(46)-Ir(1)-N(7)	91.98(13)	C(11)-N(5)-C(8)	119.3(4)
C(13)-Ir(1)-N(7)	170.60(13)	C(11)-N(5)-Ir(1)	114.3(3)
C(30)-Ir(1)-N(7)	79.14(15)	C(8)-N(5)-Ir(1)	126.0(3)
N(5)-Ir(1)-N(7)	95.47(13)	C(41)-N(6)-C(44)	119.0(3)
C(46)-Ir(1)-N(6)	79.14(14)	C(41)-N(6)-Ir(1)	126.0(3)
C(13)-Ir(1)-N(6)	97.30(14)	C(44)-N(6)-Ir(1)	113.7(3)

Table S5. Crystal data for cage **Cu_2@2** (CCDC **NO. 2376259**).

Molecular formula	$C_{51}H_{60}Cu_2IrN_{11}\cdot 2(PF_6)\cdot CH_3CN$	
Molecular weight	1497.90	
Temperature	210(2) K	
Wavelength	1.54178 Å	
Crystal system	Cubic	
Space group	I2(1)3	
Unit cell parameters	*a* = 12.2886(5) Å	α = 91.673(4)°
	b = 12.4886(4) Å	β = 108.584(4)°
	c = 17.6838(13) Å	γ = 91.691(3)°
	V =2569.1(2) Å^3	
Z	2	
F(000)	5992	
Density (calcd)	1.366 g/cm^3	
Absorption coefficient	2.645 mm^{-1}	
Theta range for data collection	2.344 to 25.000°	
Limiting indices	-14 <= h<= 14, -14 <= k<= 14, -21 <= l<= 21	
Reflections collected	97416	
Independent reflections	9035 [R(int) = 0.0632]	
Completeness to theta = 25.000°	99.8%	
Refinement method	Full-matrix least-squares on F^2	
Data / restraints / parameters	9035 / 0 / 642	
Goodness-of-fit on F^2	0.957	
Final R indices [I>2sigma(I)]	R1 = 0.0285, wR2 = 0.0895	
R indices (all data)	R1 = 0.0327, wR2 = 0.0925	
Largest diff. peak and hole	1.157 and -0.417 e.Å^{-3}	

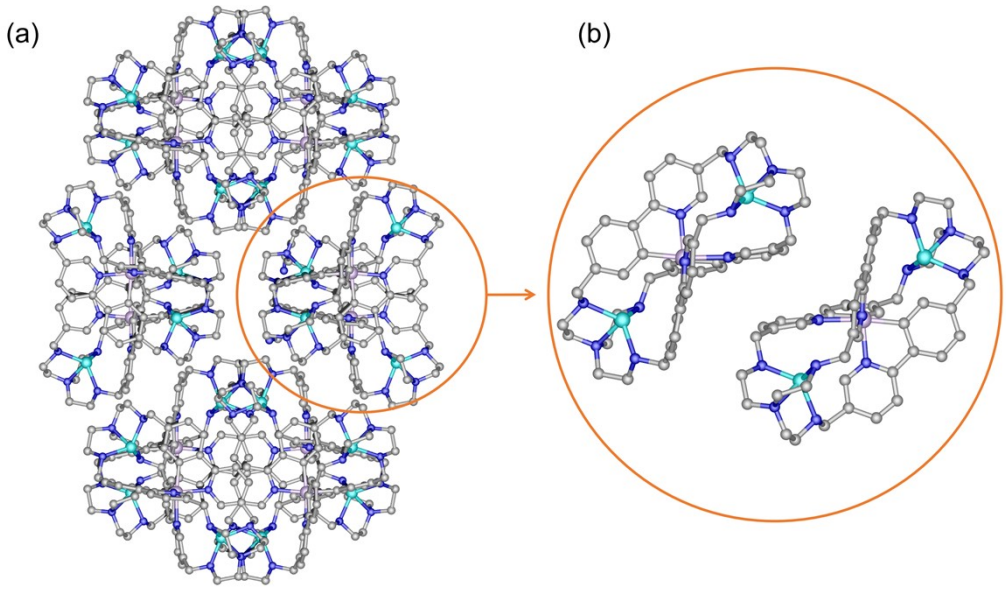

Figure S32. (a) Crystal stacking of **Cu_2@2** in *x-axis* view. (b) Circled part of **Cu_2@2** in *y-axis* view for showing the cage arrangement more clearly. Color code: C, grey; N, blue; Ir, violet, Cu, green-cyan. Hydrogen atoms, pair anions and lattice solvent molecules are omitted for clarity.

Table S6. Selected bond distances (Å) and angles (°) in **Cu_2@2**.

Bond	Length	Bond	Length
Ir(1)-C(14)#1	2.020(5)	N(1)-C(1)#1	1.442(13)
Ir(1)-C(14)#2	2.020(5)	N(1)-C(1)#2	1.442(13)
Ir(1)-C(14)	2.020(5)	N(1)-C(1)	1.442(13)
Ir(1)-N(3)	2.120(5)	N(2)-C(2)	1.469(13)
Ir(1)-N(3)#2	2.120(5)	N(2)-C(3)	1.502(12)
Ir(1)-N(3)#1	2.120(5)	N(2)-H(2)	0.9902
Cu(2)-N(4)#2	2.153(6)	N(3)-C(8)	1.325(9)
Cu(2)-N(4)#1	2.153(6)	N(3)-C(7)	1.366(8)
Cu(2)-N(4)	2.154(6)	N(4)-C(15)	1.481(10)
Cu(2)-N(5)	2.202(13)	N(4)-C(16)	1.490(10)
Cu(1)-N(2)	2.152(8)	N(4)-H(4)	0.9902
Cu(1)-N(2)#1	2.152(8)	N(5)-C(17)#2	1.465(9)
Cu(1)-N(2)#2	2.152(8)	N(5)-C(17)#1	1.465(9)
Cu(1)-N(1)	2.195(17)	N(5)-C(17)	1.465(9)
Bond	Angle	Bond	Angle
C(14)#1-Ir(1)-C(14)#2	92.4(2)	C(14)-Ir(1)-N(3)#1	94.76(19)
C(14)#1-Ir(1)-C(14)	92.4(2)	N(3)-Ir(1)-N(3)#1	94.0(2)
C(14)#2-Ir(1)-C(14)	92.4(2)	N(3)#2-Ir(1)-N(3)#1	94.0(2)
C(14)#1-Ir(1)-N(3)	169.6(2)	N(4)#2-Cu(2)-N(4)#1	118.74(7)
C(14)#2-Ir(1)-N(3)	94.76(19)	N(4)#2-Cu(2)-N(4)	118.74(7)
C(14)-Ir(1)-N(3)	79.8(2)	N(4)#1-Cu(2)-N(4)	118.74(7)
C(14)#1-Ir(1)-N(3)#2	94.77(19)	N(4)#2-Cu(2)-N(5)	83.50(18)
C(14)#2-Ir(1)-N(3)#2	79.8(2)	N(4)#1-Cu(2)-N(5)	83.50(18)
C(14)-Ir(1)-N(3)#2	169.6(2)	N(4)-Cu(2)-N(5)	83.50(18)
N(3)-Ir(1)-N(3)#2	94.0(2)	N(2)-Cu(1)-N(2)#1	118.95(8)
C(14)#1-Ir(1)-N(3)#1	79.8(2)	N(2)-Cu(1)-N(2)#2	118.95(8)
C(14)#2-Ir(1)-N(3)#1	169.6(2)	N(2)#1-Cu(1)-N(2)#2	118.95(8)

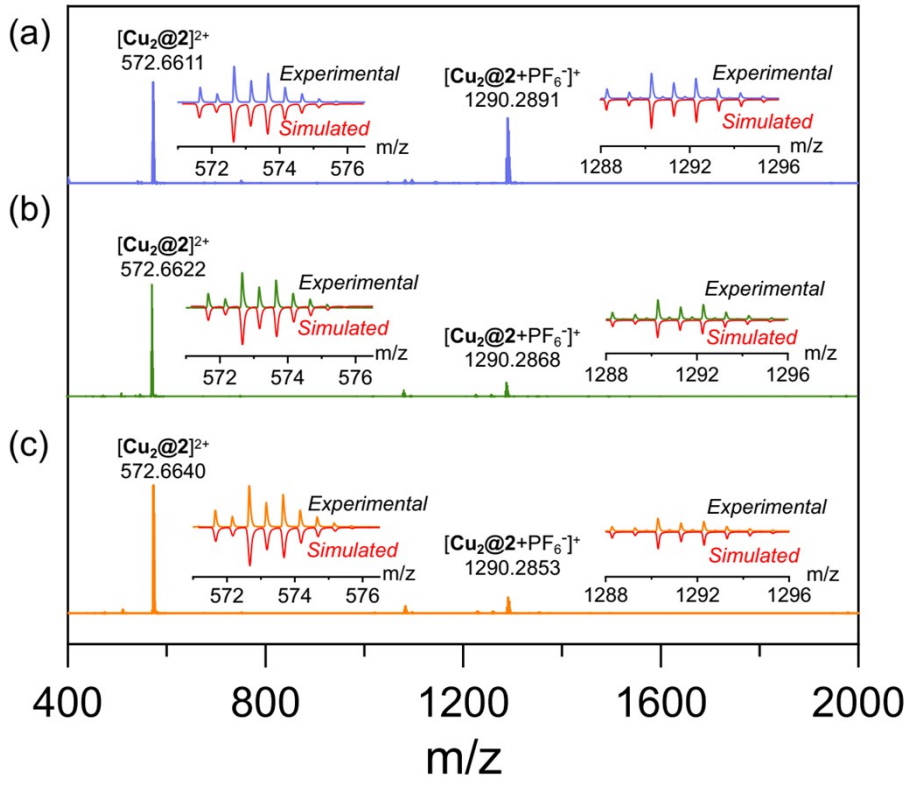

Figure S33. (a) ESI-TOF-MS spectra of **Cu_2@2** in methanol solvent as synthesized. (b) ESI-TOF-MS spectra of **Cu_2@2** in methanol solvent exposed to air after one week. (c) ESI-TOF-MS spectra of **Cu_2@2** after bubbling O_2 in methanol solvent.

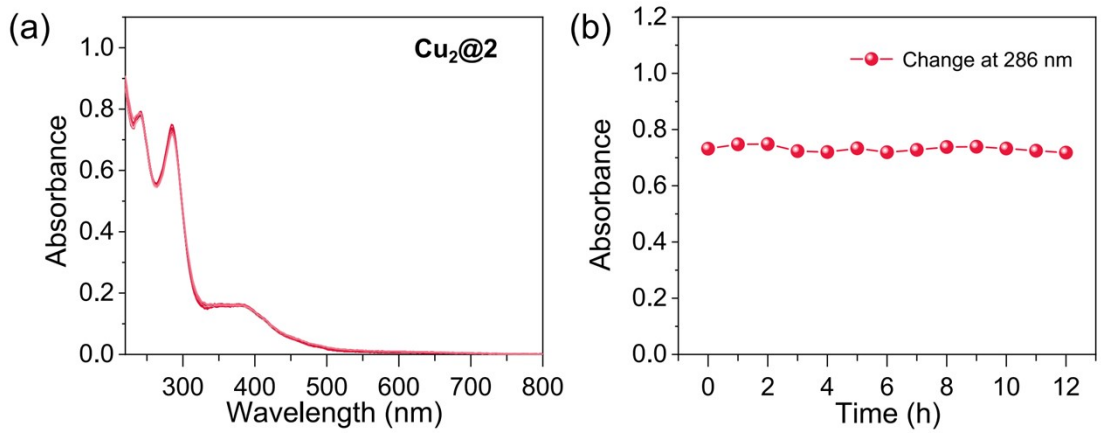

Figure S34. (a) Evolution of the UV-Vis spectra of **Cu_2@2** in CH_3CN upon the irradiation of 450 nm LED for 0-12 h; (b) Time-dependent corresponding absorption of **Cu_2@2** at 286 nm upon the irradiation of 450 nm LED.

4. Data Relative to C(sp^3)-H photo-oxidation

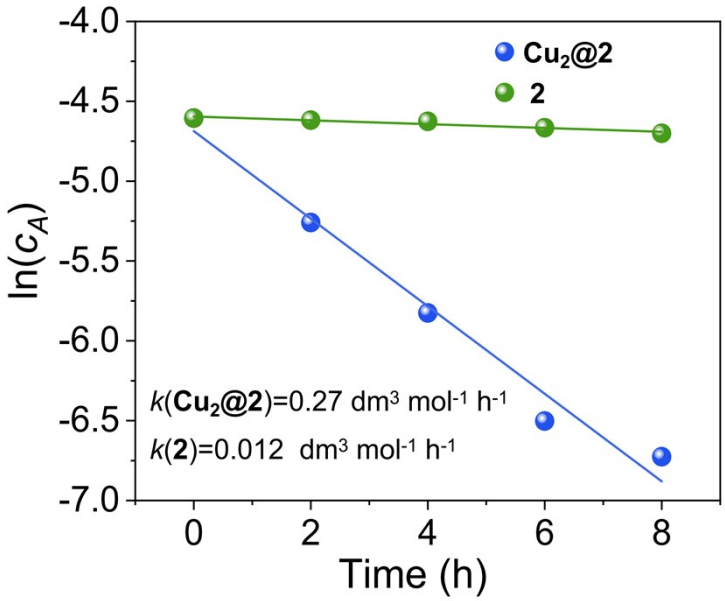

Figure S35. First order kinetics fits of C(sp^3)−H oxidation by **Cu$_2$@2** (blue line) and cage **2** (green line) under optimized conditions

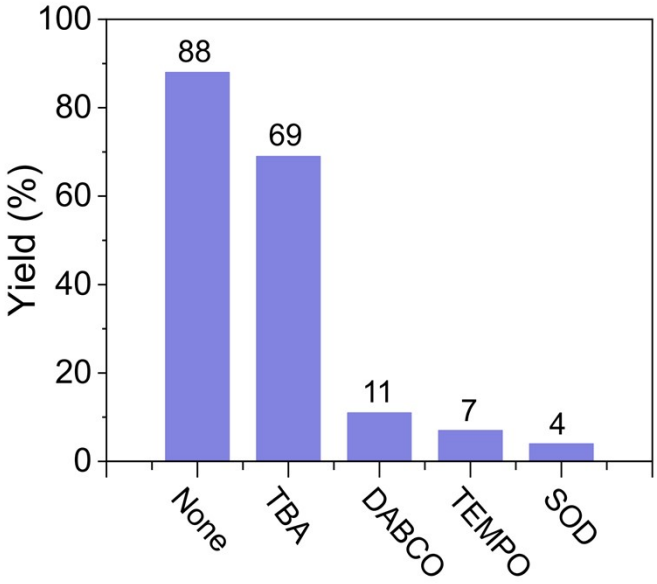

Figure S36. Effect of scavengers on the photocatalytic oxidative **1a** over **Cu$_2$@2**.

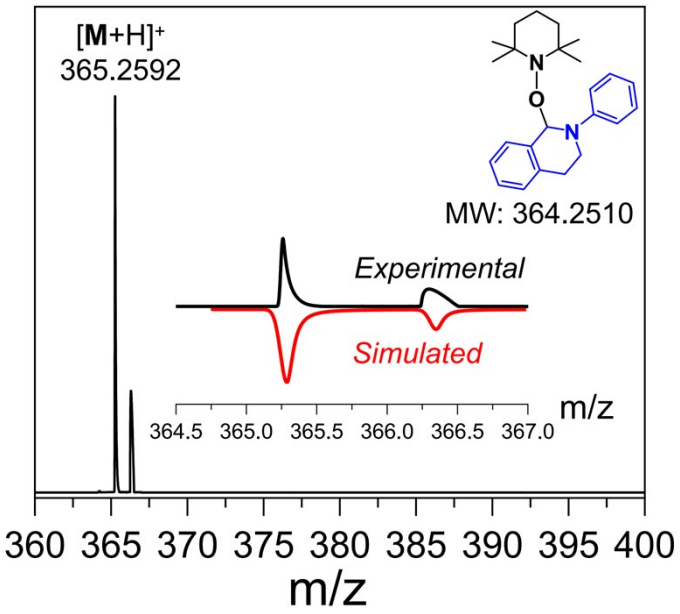

Figure S37. TEMPO trapping experiment. Reaction conditions: N-phenyl tetrahydroisoquinoline (0.1 equiv., 0.02 mmol), **Cu_2@2** (5 mol%), TEMPO (0.2 equiv., 0.06 mmol), in acetonitrile (2.0 mL) under irradiation with a 450 nm LED for 12 h. After reaction, the mixture was filtered and submitted to mass spectrometry (ESI-TOF-MS) and the TEMPO trapped product was found. HRMS (ESI) m/z calcd. for $[M+H]^+$ 365.2510, found 365.2592.

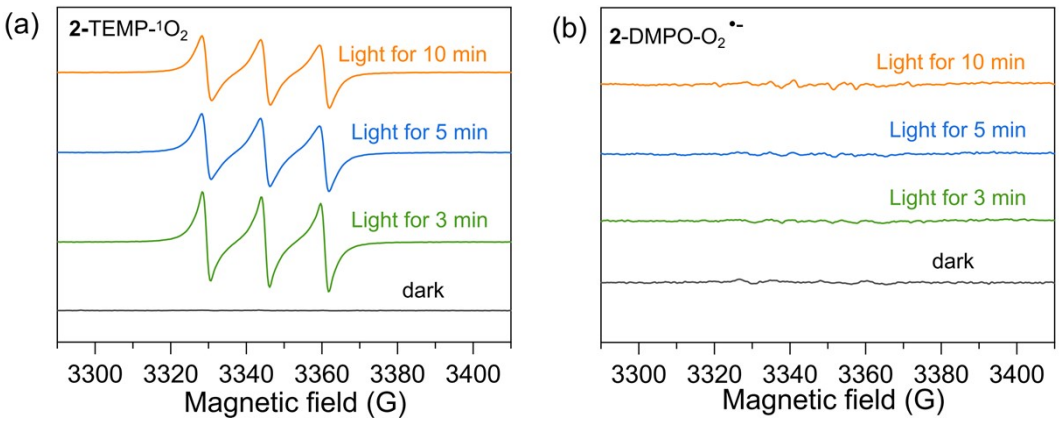

Figure S38. (a) the detection of $^1O_2$ in a mixture of TEMP and 1.0 μM cage **2** in acetone solution under xenon lamp irradiation using EPR spectra in an air atmosphere; (b) the detection of $O_2^{\bullet-}$ in a mixture of 30.0 μL DMPO and 1.0 μmol cage **2** in methanol solution under xenon lamp irradiation using EPR spectra in an air atmosphere.

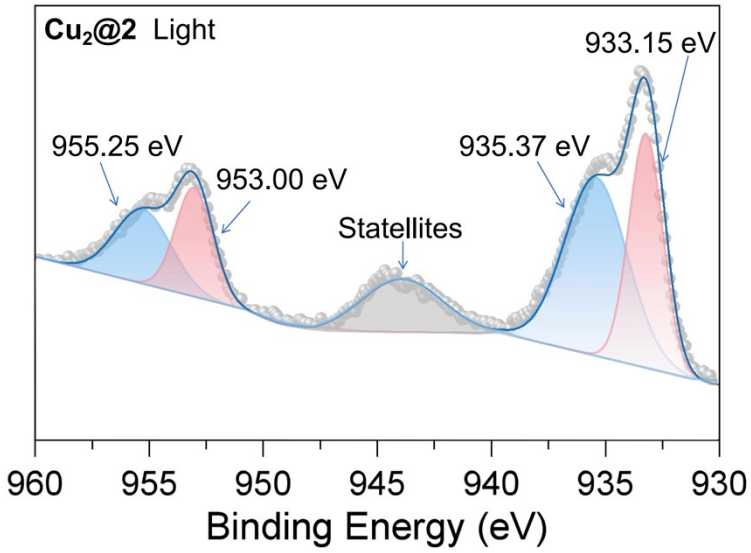

Figure S39. X-ray photoelectron spectroscopy (XPS) spectra of **Cu_2@2** after illumination with 450 nm LED, showing the Cu_{2p} signal with two fitting peaks at 953.00 eV and 933.15 eV for Cu(I) ions, as well as, 955.25 eV and 935.37 eV for Cu(II) ions.

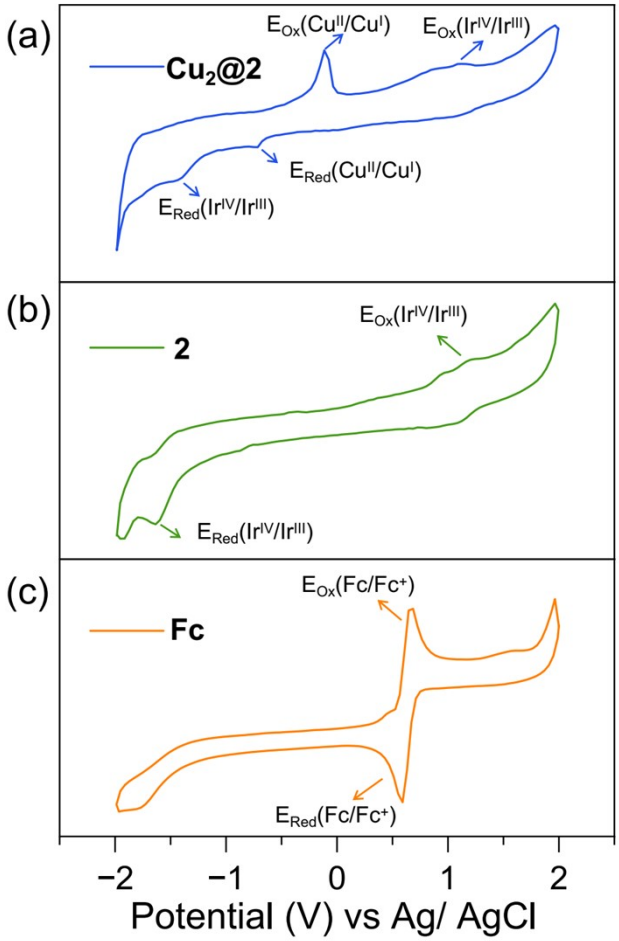

Figure S40. Cyclic voltammograms of (a) **Cu_2@2**, (b) **2** and (c) **Fc** in dry CH_3CN solution containing 0.1 M *n*-Bu_4NPF_6 under a N_2 atmosphere.

Cyclic voltammetry measurements of **Cu_2@2** showed peaks of -0.07 and -0.71 (V *vs* Ag/AgCl) redox couples for Cu^{II}/Cu^{I}, and the couples of +1.20 and -1.50 (V *vs* Ag/AgCl) for Ir^{IV}/Ir^{III}.[6-9]

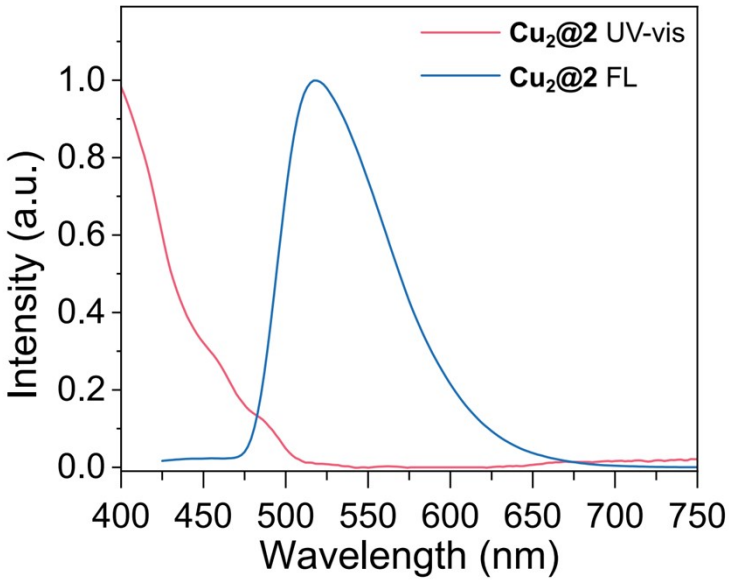

Figure S41. Normalized absorption and emission spectra of **Cu_2@2** ($E_{0\text{-}0}$ = 2.55 eV). The Method of Calculation of the Excited-State Reduction Potential: $E_{Red^*}(Ir^{IV}/Ir^{III*}) = E_{Ox}(Ir^{IV}/Ir^{III}) – E_{0\text{-}0}$ = +1.20 - 2.55 = -1.35 (V *vs* Ag/AgCl).

5. Synthesis of substrates

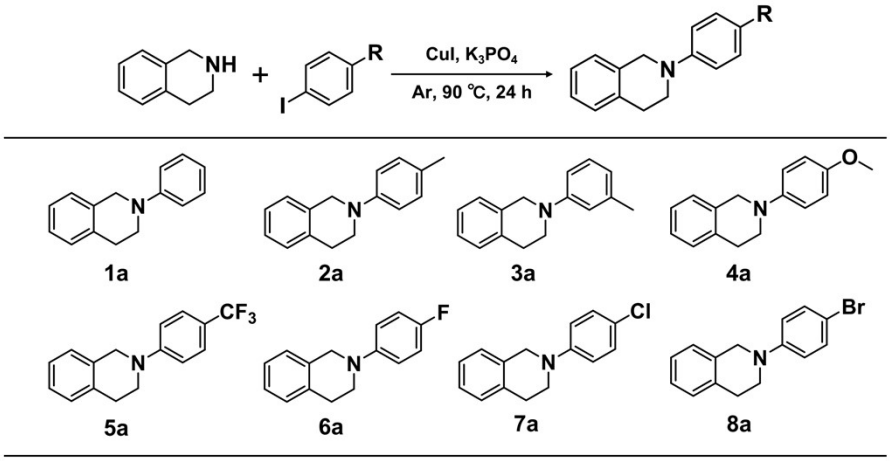

Scheme S5. The synthetic routes of substrates.

The substrates 1-7a were synthesized as reported [10-12]: Copper(I) iodide (200 mg, 1.05 mmol, 10 mol%) and potassium phosphate (4.25 g, 20.0 mmol, 2 equiv.) were put into a Schlenk tube. The tube was evacuated and back filled with Ar. 2-Propanol (10.0 mL), ethylene glycol (1.1 mL, 20.0 mmol, 2 equiv.), 1,2,3,4-tetrahydroisoquinoline (2.0 mL, 15 mmol, 1.5 equiv.) and iodobenzene derivative (10.0 mmol, 1 equiv.) were added successively at room temperature. The reaction mixture was heated at 90 °C and kept for 24 h and then allowed to cool to room temperature. Diethyl ether (20 mL) and water (20 mL) were then added to the reaction mixture. The organic layer was extracted by diethyl ether (2 × 20 mL). The combined organic phases were washed with brine and dried over magnesium sulfate. The solvent was removed by rotary evaporation and purified by column chromatography on silica gel (petroleum ether; petroleum ether/ dichloromethane) to give the pure products.

^{1}H NMR spectra of substrates

2-phenyl-1,2,3,4-tetrahydroisoquinoline (1a) ^{1}H NMR (400 MHz, Chloroform-d) δ 7.34 – 7.23 (m, 2H), 7.21 – 7.14 (m, 4H), 7.03 – 6.95 (m, 2H), 6.88 – 6.74 (m, 1H), 4.42 (s, 2H), 3.57 (t, J = 5.9 Hz, 2H), 3.00 (d, J = 5.8 Hz, 2H), 1.55 (s, 2H).

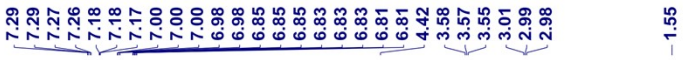

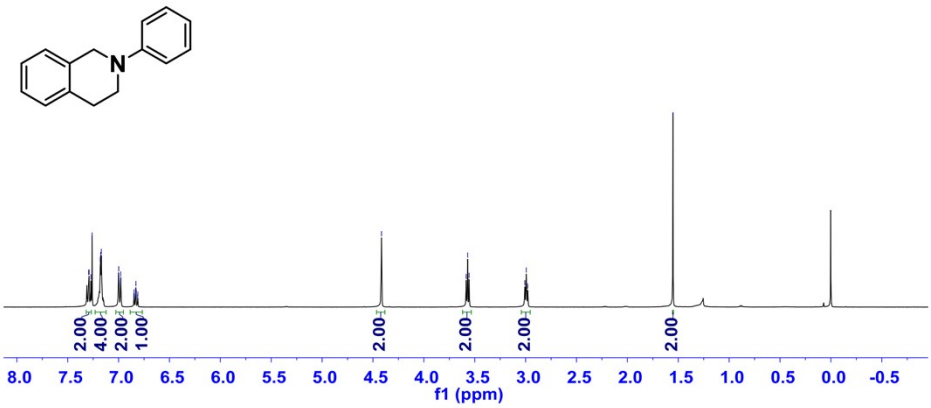

2-(p-tolyl)-1,2,3,4-tetrahydroisoquinoline (2a). ^{1}H NMR (400 MHz, Chloroform-d) δ 7.20 - 7.13 (m, 4H), 7.09 (s, 2H), 6.92 (d, J = 8.6 Hz, 2H), 4.36 (s, 2H), 3.51 (t, J = 5.9 Hz, 2H), 2.99 (s, 2H), 2.28 (s, 3H).

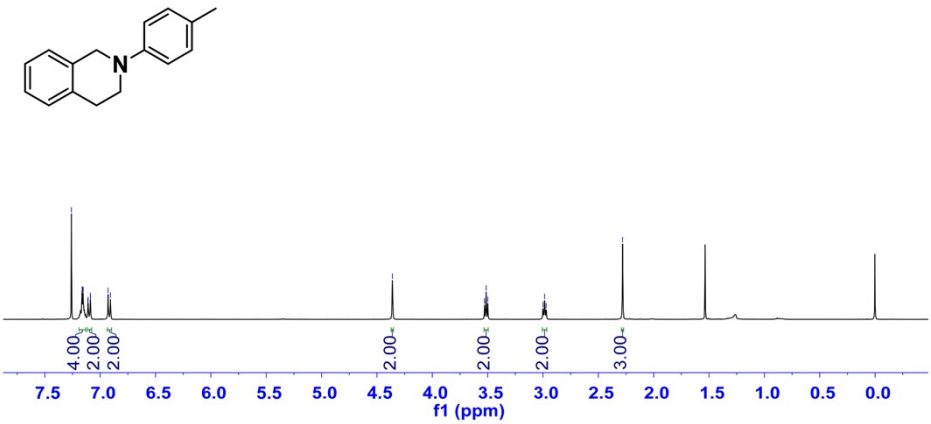

2-(m-tolyl)-1,2,3,4-tetrahydroisoquinoline (3a). ^{1}H NMR (400 MHz, Chloroform-*d*) *δ* 7.42 – 7.12 (m, 1H), 6.87 (s, 0H), 6.72 (d, *J* = 7.4 Hz, 0H), 4.46 (s, 0H), 3.60 (d, *J* = 5.8 Hz, 0H), 3.05 (d, *J* = 5.9 Hz, 0H), 2.41 (s, 1H).

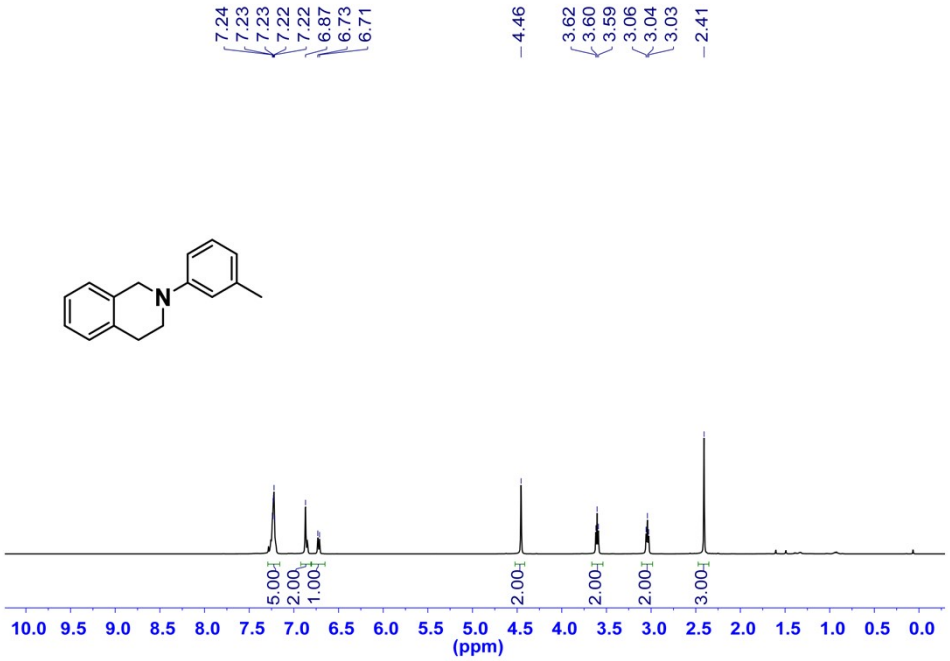

2-(4-methoxyphenyl)-1,2,3,4-tetrahydroisoquinoline (4a) ^{1}H NMR (400 MHz, Chloroform-d) *δ* 7.28 (s, 1H), 7.19 (s, 4H), 7.00 (s, 2H), 6.91 (s, 2H), 4.33 (s, 2H), 3.81 (s, 3H), 3.48 (s, 2H), 3.02 (t, *J* = 5.9 Hz, 2H).

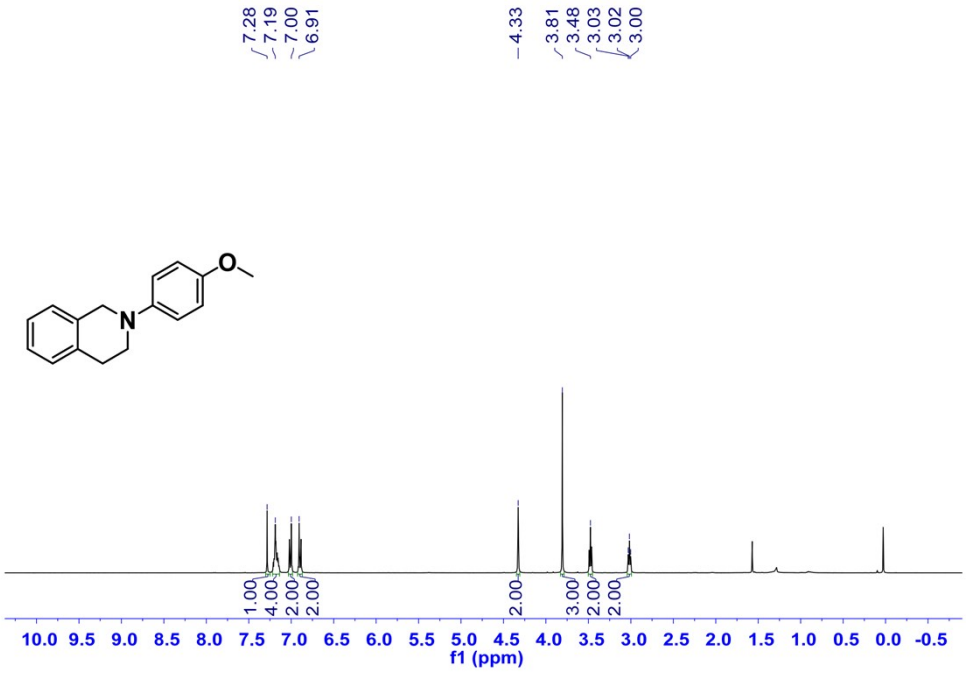

2-(4-(trifluoromethyl)phenyl)-1,2,3,4-tetrahydroisoquinoline (5a) ^{1}H NMR (400 MHz, Chloroform-d) *δ* 7.55 (d, J = 8.5 Hz, 2H), 7.24 (d, J = 6.8 Hz, 4H), 6.97 (d, J = 8.6 Hz, 2H), 4.52 (s, 2H), 3.66 (s, 2H), 3.03 (s, 2H).

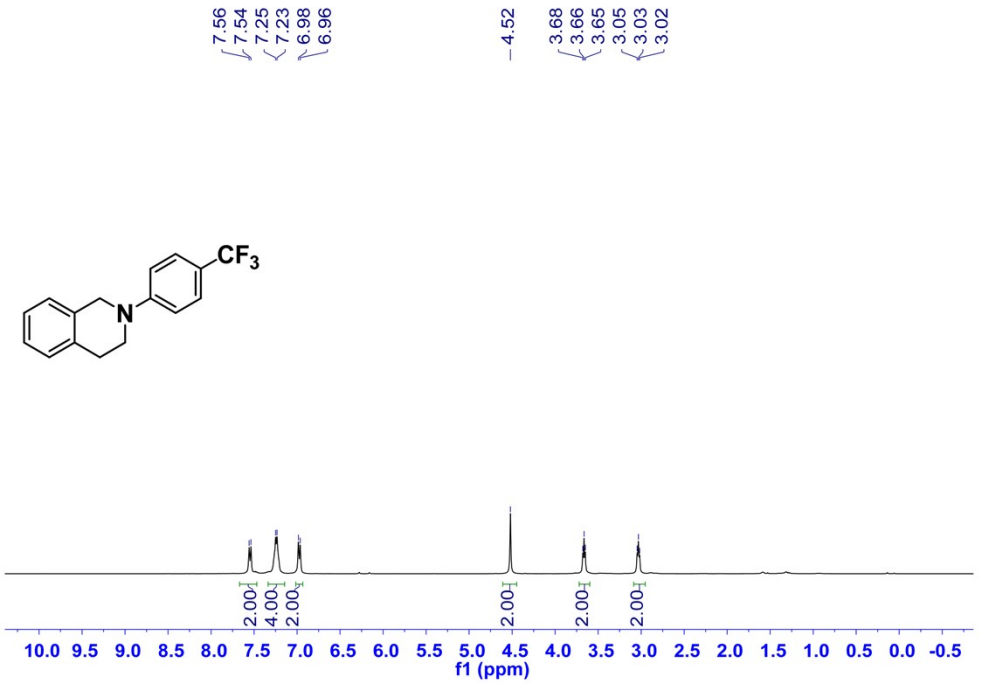

2-(4-fluorophenyl)-1,2,3,4-tetrahydroisoquinoline (6a). ^{1}H NMR (400 MHz, Chloroform-d) *δ* 7.28 (ddt, *J* = 12.8, 8.0, 3.9 Hz, 4H), 7.17 – 6.90 (m, 4H), 4.42 (s, 2H), 3.57 (t, *J* = 5.9 Hz, 2H), 3.08 (t, *J* = 5.9 Hz, 2H).

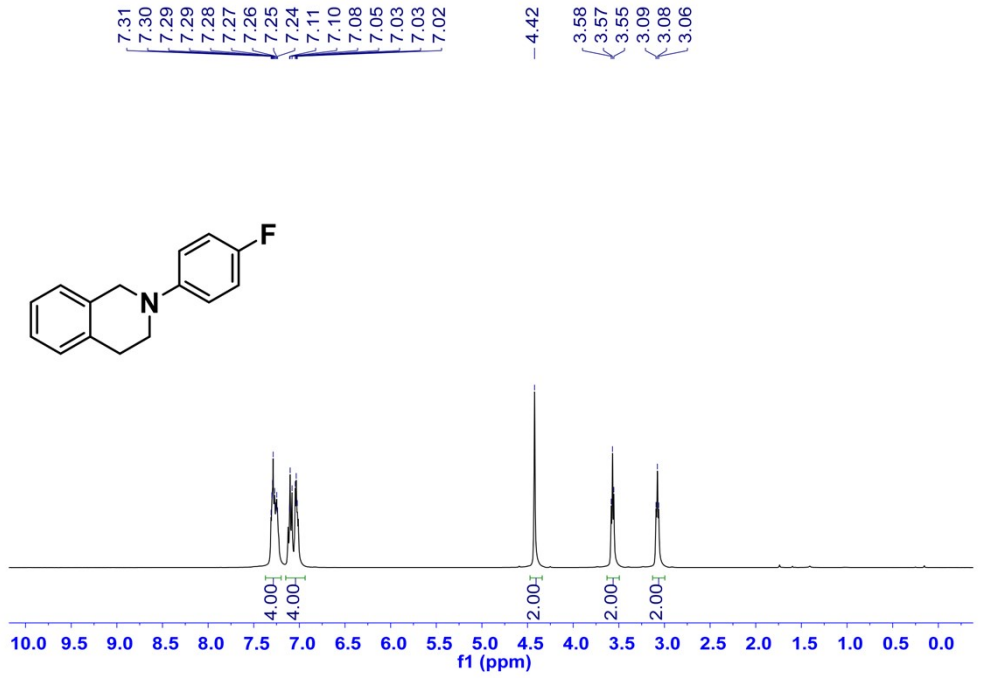

2-(4-chlorophenyl)-1,2,3,4-tetrahydroisoquinoline (7a). ^{1}H NMR (400 MHz, Chloroform-d) *δ* 7.25 (dt, *J* = 16.7, 6.8 Hz, 6H), 6.93 (d, *J* = 8.7 Hz, 2H), 4.42 (s, 2H), 3.57 (s, 2H), 3.04 (d, *J* = 5.9 Hz, 2H).

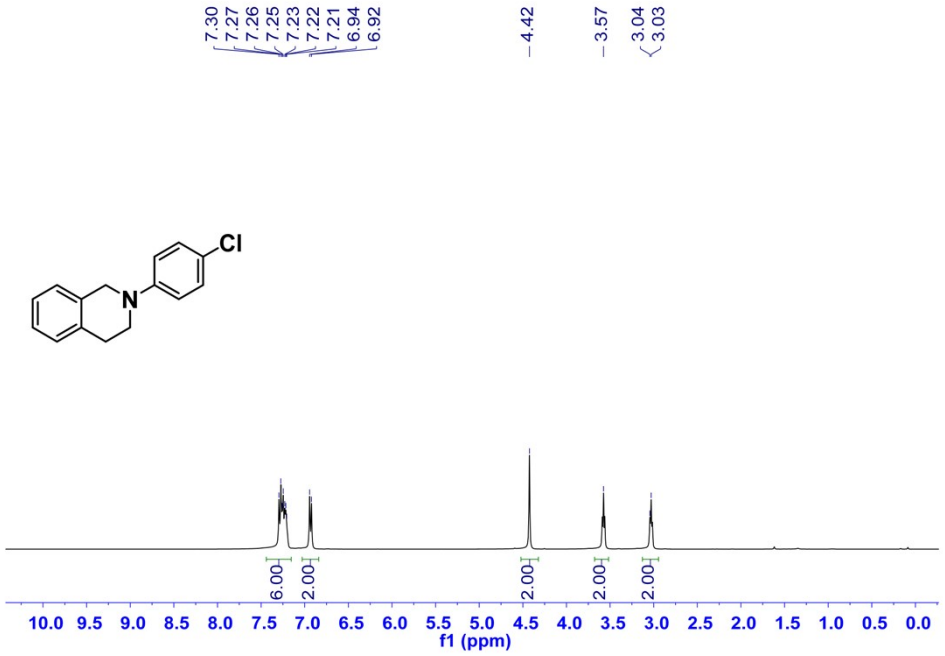

2-(4-bromophenyl)-1,2,3,4-tetrahydroisoquinoline (8a) ^{1}H NMR (400 MHz, Chloroform-*d*) *δ* 7.44 – 7.33 (m, 2H), 7.26 – 7.14 (m, 4H), 7.02 – 6.77 (m, 2H), 4.41 (s, 2H), 3.56 (t, *J* = 5.8 Hz, 2H), 3.01 (s, 2H).

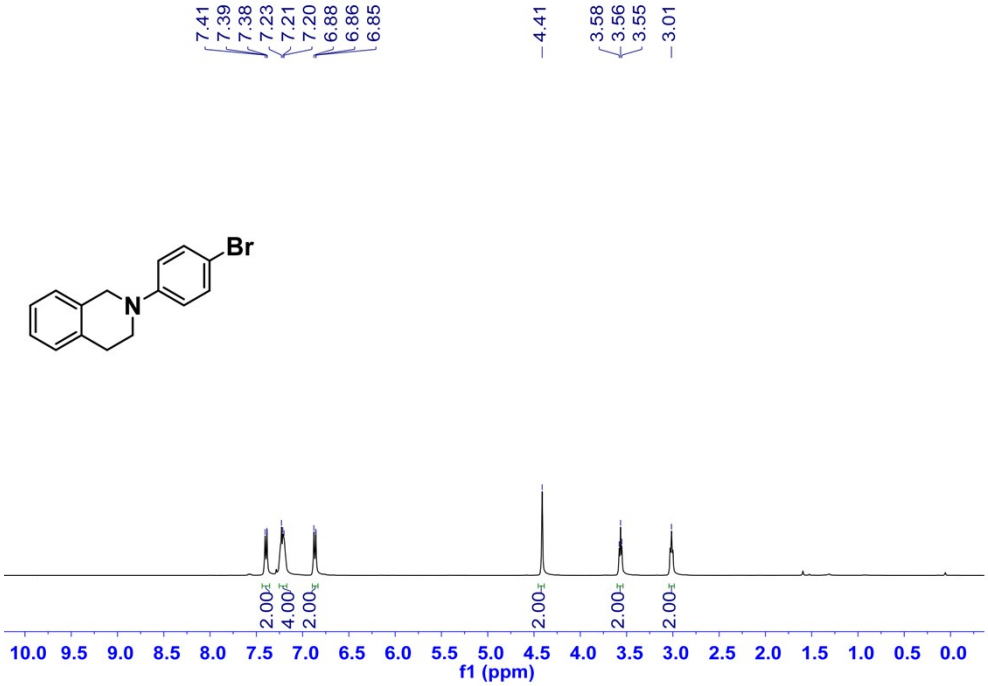

6. ^{1}H NMR spectra of catalytic products

2-phenyl-2,3-dihydroisoquinolin-4(1H)-one (1b). ^{1}H NMR (400 MHz, Chloroform-d) δ 8.19 (dd, J = 7.7, 1.4 Hz, 1H), 7.52 – 7.46 (m, 1H), 7.45 – 7.38 (m, 5H), 7.28 (d, J = 1.4 Hz, 2H), 4.02 (t, J = 6.5 Hz, 2H), 3.17 (t, J = 6.4 Hz, 2H).

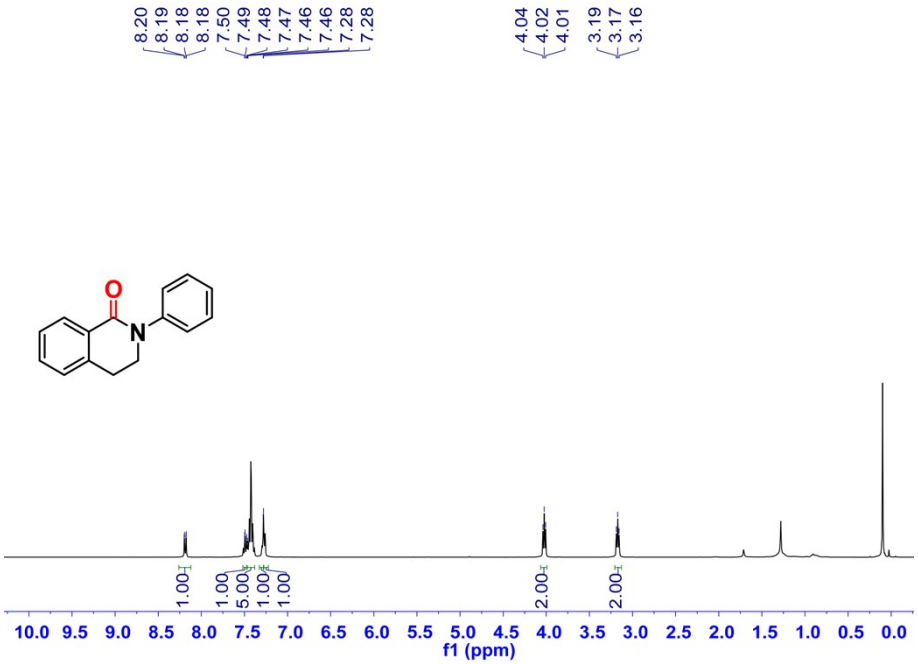

2-(p-tolyl)-2,3-dihydroisoquinolin-4(1H)-one (2b). ^{1}H NMR (400 MHz, Chloroform-*d*) δ 8.18 (dd, J = 7.6, 1.4 Hz, 1H), 7.48 (dd, J = 7.5, 1.5 Hz, 1H), 7.41 (dd, J = 7.7, 1.3 Hz, 1H), 7.33 – 7.21 (m, 5H), 4.07 – 3.92 (m, 2H), 3.16 (t, J = 6.5 Hz, 2H), 2.39 (s, 3H).

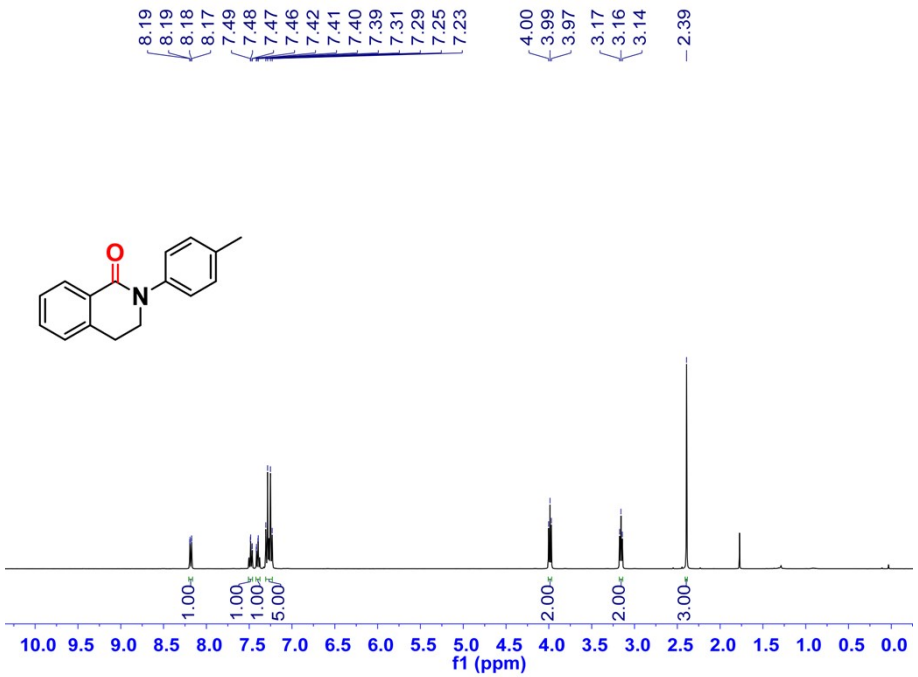

2-(m-tolyl)-3,4-dihydroisoquinolin-1(2H)-one (3b). ^{1}H NMR (400 MHz, Chloroform-*d*) *δ* 8.18 (s, 1H), 7.48 (dd, *J* = 7.4, 1.5 Hz, 1H), 7.44 - 7.37 (m, 1H), 7.33 (t, *J* = 7.8 Hz, 1H), 7.30 - 7.27 (m, 1H), 7.27 - 7.23 (m, 1H), 7.23 - 7.17 (m, 1H), 7.10 (d, *J* = 7.6 Hz, 1H), 4.13 - 3.88 (m, 2H), 3.55 (t, *J* = 4.4 Hz, 1H), 3.16 (t, *J* = 6.5 Hz, 2H), 2.41 (s, 3H).

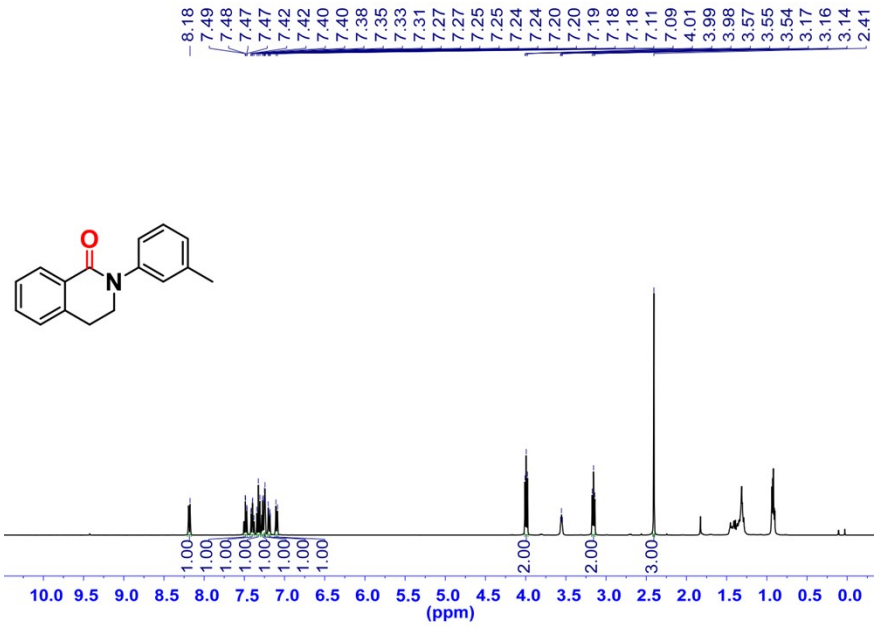

2-(4-methoxyphenyl)-2,3-dihydroisoquinolin-4(1H)-one (4b). ^{1}H NMR (400 MHz, Chloroform-*d*) δ 8.16 (s, 1H), 7.52 – 7.46 (m, 1H), 7.39 (t, *J* = 7.5 Hz, 1H), 7.35 – 7.30 (m, 2H), 7.29 – 7.24 (m, 1H), 7.02 – 6.92 (m, 2H), 3.97 (t, *J* = 6.5 Hz, 2H), 3.85 (d, *J* = 1.0 Hz, 3H), 3.16 (t, *J* = 6.5 Hz, 2H).

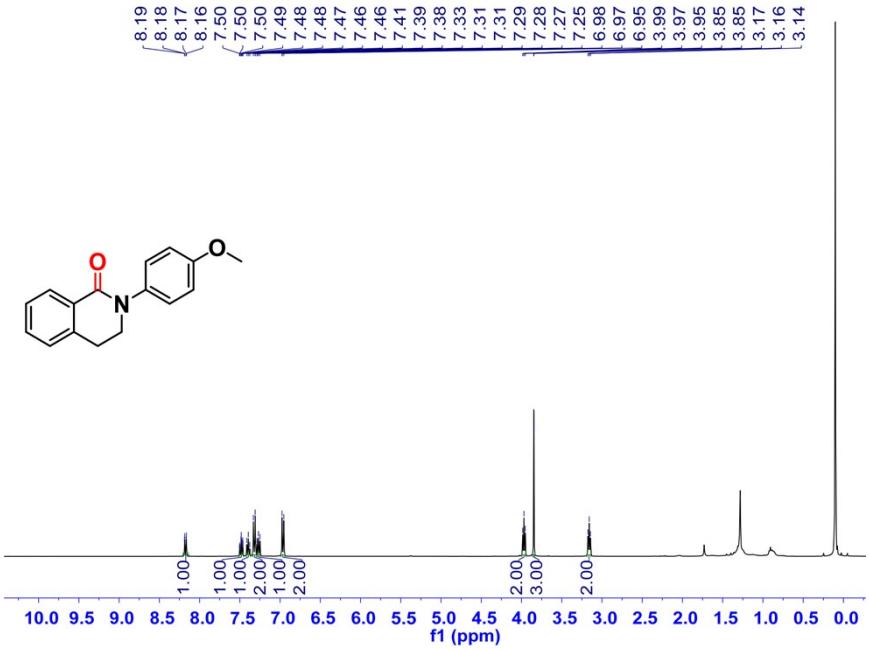

2-(4-(trifluoromethyl)phenyl)-2,3-dihydroisoquinolin-4(1H)-one (5b). ^{1}H NMR (400 MHz, Chloroform-d) *δ* 8.18 (dd, *J* = 7.7, 1.3 Hz, 1H), 7.69 (d, *J* = 8.5 Hz, 2H), 7.57 (d, *J* = 8.4 Hz, 2H), 7.51 (dd, *J* = 7.4, 1.5 Hz, 1H), 7.42 (d, *J* = 1.2 Hz, 1H), 7.35 – 7.20 (m, 2H), 4.06 (t, *J* = 6.4 Hz, 2H), 3.19 (t, *J* = 6.4 Hz, 2H).

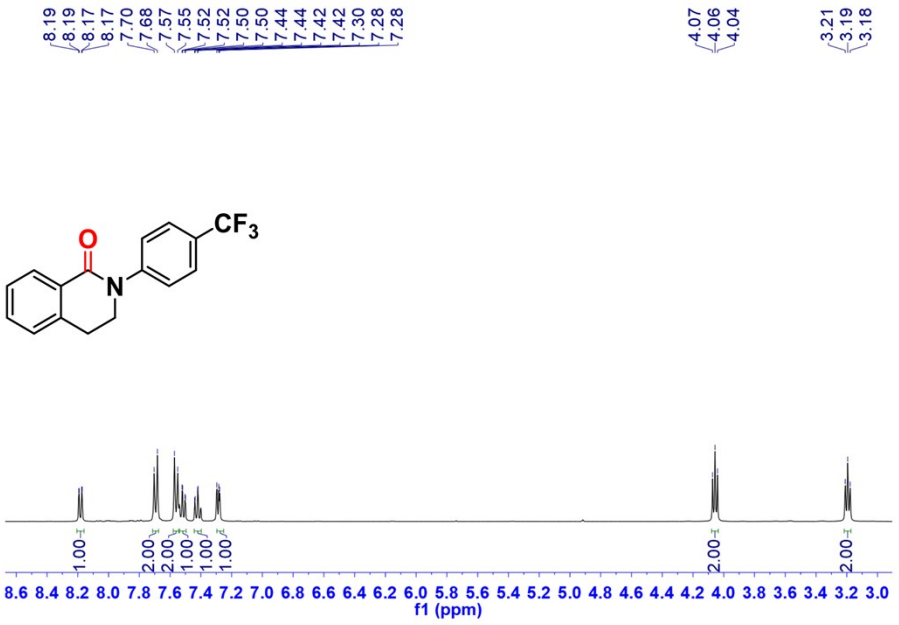

2-(4-fluorophenyl)-2,3-dihydroisoquinolin-4(1H)-one (6b). ^{1}H NMR (400 MHz, Chloroform-*d*) *δ* 8.17 (dd, *J* = 7.7, 1.4 Hz, 1H), 7.49 (dd, *J* = 7.5, 1.5 Hz, 1H), 7.38 (ddd, *J* = 11.6, 6.4, 2.9 Hz, 3H), 7.32 – 7.18 (m, 1H), 7.12 (t, *J* = 8.6 Hz, 2H), 4.06 – 3.75 (m, 2H), 3.17 (t, *J* = 6.4 Hz, 2H).

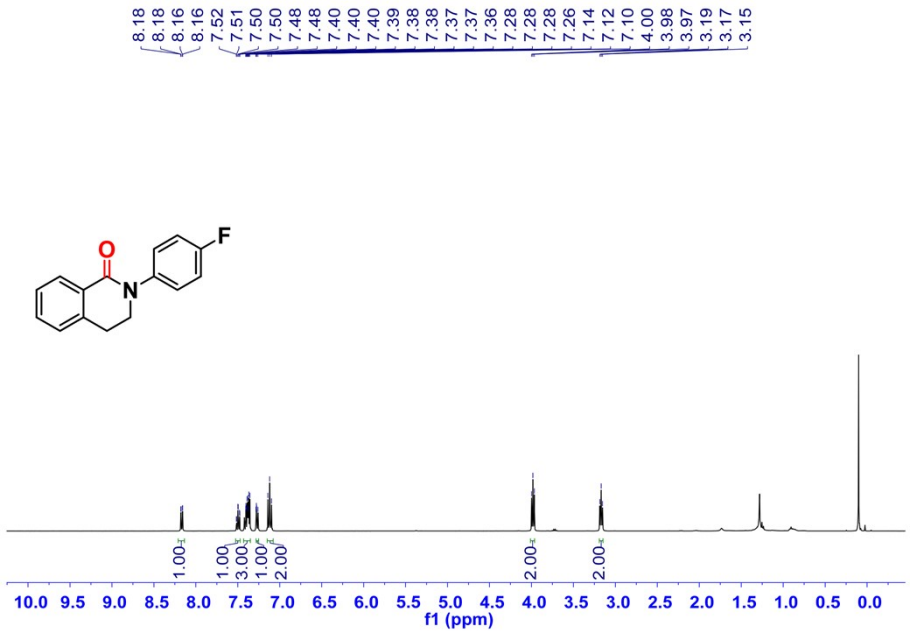

2-(4-chlorophenyl)-2,3-dihydroisoquinolin-4(1H)-one (7b). ^{1}H NMR (400 MHz, Chloroform-*d*) δ 8.17 (dd, *J* = 7.7, 1.3 Hz, 1H), 7.49 (dd, *J* = 7.5, 1.4 Hz, 1H), 7.38 (d, *J* = 8.3 Hz, 5H), 7.28 (d, *J* = 1.9 Hz, 1H), 4.00 (t, *J* = 6.5 Hz, 2H), 3.17 (t, *J* = 6.4 Hz, 2H).

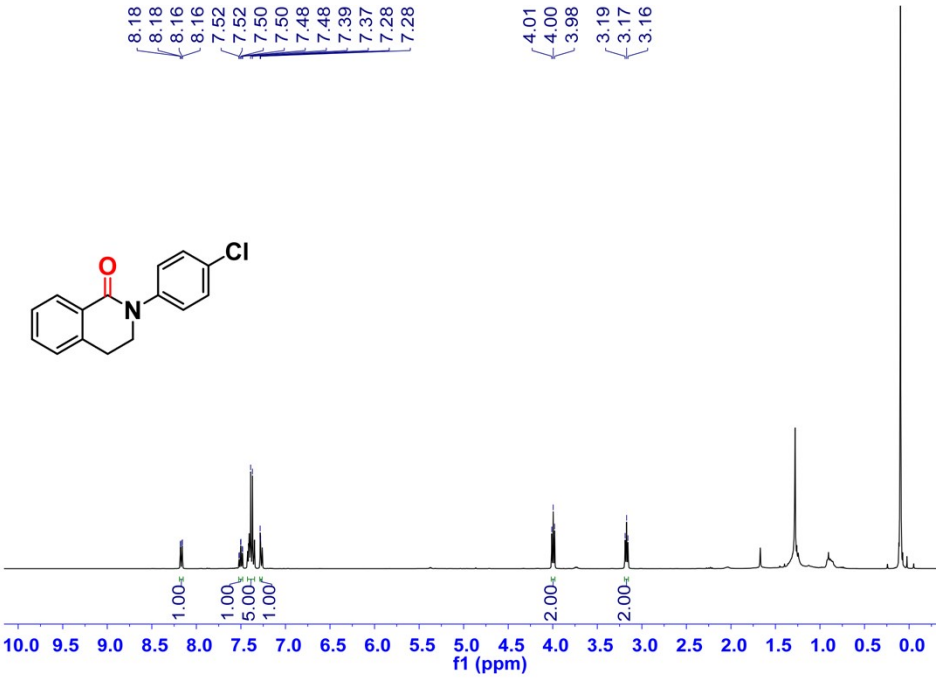

2-(4-bromophenyl)-2,3-dihydroisoquinolin-4(1H)-one (8b). ^{1}H NMR (400 MHz, Chloroform-*d*) δ 8.20 – 8.10 (m, 1H), 7.55 (d, *J* = 8.7 Hz, 2H), 7.50 (d, *J* = 1.5 Hz, 1H), 7.42 (dd, *J* = 7.6, 1.2 Hz, 1H), 7.31 (d, *J* = 8.7 Hz, 3H), 3.99 (t, *J* = 6.5 Hz, 2H), 3.17 (s, 2H).

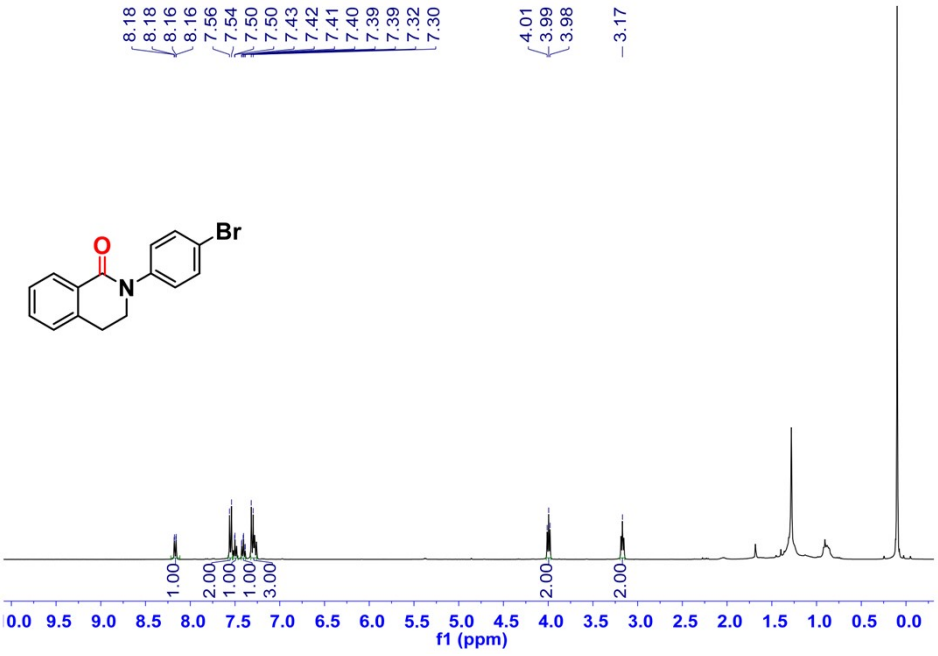

7. Reference

1 SMART, Data collection software (version 5.629) (Bruker AXS Inc., Madison, WI, 2003).

2 SAINT, Data reduction software (version 6.54) (Bruker AXS Inc., Madison, WI, 2003).

3 G. M. Sheldrick, SHELXTL97, Program for crystal structure solution (University of Göttingen: Göttingen, Germany, 1997).

4 Z. Almansaf, J. Hu, F. Zanca, H. R. Shahsavari, B. Kampmeyer, M. Tsuji, K. Maity, V. Lomonte, Y. Ha, P. Mastrorilli, S. Todisco, M. Benamara, R. Oktavian, A. Mirjafari, P. Z. Moghadam, A. R. Khosropour and H. Beyzavi, *ACS Applied Materials & Interfaces*, 2021, **13**, 6349.

5. M. Boiocchi, M. Bonizzoni, L. Fabbrizzi, G. Piovani and A. Taglietti, A Dimetallic Cage with a Long Ellipsoidal Cavity for the Fluorescent Detection of Dicarboxylate Anions in Water, *Angew. Chem. Int. Ed.*, 2004, **43**, 3847.

6. T. Fujii, S. Yamaguchi, Y. Funahashi, T. Ozawa, T. Tosha, T. Kitagawa and H. Masuda, Mononuclear Copper(II)-Hydroperoxo Complex Derived from Reaction of Copper(I) Complex with Dioxygen as a Model of DβM and PHM, *Chem. Commun.*, 2006, **42**, 4428.

7 G. D. Leener, D. Over, C. Smet, D. Cornut, A. G. Porras-Gutierrez, I. López, B. Douziech, N. Le Poul, F. Topić, K. Rissanen, Y. L. Mest, I. Jabin and O. Reinaud, “Two-Story” Calix[6]arene-Based Zinc and Copper Complexes: Structure, Properties, and O_2 Binding, *Inorg. Chem.*, 2017, **56**, 10971.

8 J. H. Shon, S. Sittel and T. S. Teets, Synthesis and Characterization of Strong Cyclometalated Iridium Photoreductants for Application in Photocatalytic Aryl Bromide Hydrodebromination, *ACS Catal.* 2019, **9**, 8646.

9 J. A. Willms, H. Gleich, M. Schrempp, D. Menche, M. Engeser, Investigations of the Copper-Catalyzed Oxidative Cross-Coupling of Tetrahydroisoquinolines with Diethylzinc by a Combination of Mass Spectrometric and Electrochemical Methods, *Chem. Eur. J.* 2018, **24**, 2663.

10. X. Z. Shu, X. F. Xia, Y. F. Yang, K. G. Ji, X. Y. Liu, Y. M. Liang, Selective Functionalization of sp^3 C−H Bonds Adjacent to Nitrogen Using (Diacetoxyiodo)benzene (DIB), *J. Org. Chem.*, 2009, **74**, 7464.

11. A. Tanoue, W. J. Yoo, S. Kobayashi, Sulfuryl Chloride as an Efficient Initiator for the Metal-Free Aerobic Cross-Dehydrogenative Coupling Reaction of Tertiary Amines, *Org Lett.*, 2014, **16**, 2346.

12. H. E. Ho, Y. Ishikawa, N. Asao, Y. Yamamoto, T. Jin, Highly Efficient Heterogeneous Aerobic Cross-dehydrogenative Coupling via C−H Functionalization of Tertiary Amines Using a Nanoporous Gold Skeleton Catalyst, *Chem. Commun.*, 2015, **51**, 12764.